

17

Cyanuric Acid and Melamine: A Platform for the Construction of Soluble Aggregates and Crystalline Materials

ERIC E. SIMANEK, XINHUA LI, INSUNG S. CHOI, and
GEORGE M. WHITESIDES
Harvard University, Cambridge, MA, USA

17.1	INTRODUCTION	
17.1.1	Ion Receptors	596
17.1.2	Small Molecule Receptors	596
17.1.3	Molecular "Machines"	596
17.1.4	Multiparticle Aggregates	596
17.2	OUR WORK	599
17.3	CA-M	599
17.3.1	Hydrogen Bonds	599
17.3.2	Symmetries	600
17.3.3	Synthesis	601
17.4	ORGANIZATION OF THIS CHAPTER	602
17.5	SOLUBLE AGGREGATES	602
17.5.1	Design	602
17.5.1.1	The effect of preorganization on the translational entropy (ΔS_{trans}) of assembly	602
17.5.1.2	The effect of preorganization on rotational entropy (ΔS_{rot})	605
17.5.1.3	The effect of preorganization on conformational entropy (ΔS_{conf})	605
17.5.1.4	Peripheral crowding	605
17.5.2	Characterization	605
17.5.2.1	Stoichiometry	606
17.5.2.2	The determination of molecular weight: vapor phase osmometry	607
17.5.2.3	The determination of molecular weight: gel permeation chromatography	607
17.5.2.4	The determination of molecular weight: electrospray ionization mass spectrometry	608
17.5.2.5	Relative stability: methanol titrations	608
17.5.2.6	Relative stability: analysis of the GPC trace	609
17.5.2.7	^1H and ^{13}C NMR spectroscopies	609
17.5.2.8	Isomerism	610
17.5.3	Computation	612
17.5.3.1	Starting point for the calculations and minimization strategy	614
17.5.3.2	The role of solvent	614
17.5.4	Theory	615
17.5.4.1	The number of hydrogen bonds (HB) is proportional to the enthalpy of aggregation (ΔH)	615
17.5.4.2	The number of particles is proportional to the entropy of aggregation	615
17.6	CRYSTALLINE SOLIDS	616
17.6.1	Crystal Engineering	616

17.6.2	Motifs and Structure	616
17.6.2.1	Linear tapes: small peripheral groups	616
17.6.2.2	Crinkled tapes: medium-sized peripheral groups	618
17.6.2.3	Rosette: large peripheral groups	618
17.6.3	Implications for Crystal Engineering	618
17.6.3.1	Cocrystallization is difficult	618
17.6.3.2	Conformational complexity and polymorphism	619
17.6.3.3	The utility of powder diffraction	619
17.7	CONCLUSIONS	619
17.8	REFERENCES	620

17.1 INTRODUCTION

This chapter summarizes efforts to construct soluble aggregates and crystalline materials utilizing the noncovalent interactions (principally hydrogen bonds) between derivatives of cyanuric acid (CA) and melamine (M). The discussion is divided into two parts: soluble aggregates and crystalline materials.

Organic chemistry is turning from the synthesis of covalent molecules to the assembly of noncovalent aggregates. This shift in interest reflects both a high degree of mastery of covalent synthesis, and realization of the importance of noncovalent interactions. The dissection of natural systems—exemplified by Mrksich and Dervan's examination of *ds*DNA-distamycin derivatives,¹ Schreiber's study of FK-506-FKBP,² and Williams *et al.*'s inquiries into vancomycin-D-Ala-D-Ala³—has begun to clarify their structural and thermodynamic foundations. The specificity of these naturally occurring systems is not matched by design-based efforts of the type pioneered by Pedersen,⁴ Cram,⁵ and Lehn.⁶ These efforts have, nonetheless, produced increasing numbers of aggregates of different classes.

The design of noncovalent aggregates is now a central challenge for organic chemistry. By keeping the number of particles and/or the number of different types of noncovalent interactions to a manageable number, it is beginning to be possible to develop general principles of self-assembly. While several classes of designed assemblies have been explored, four main classes have emerged as foci for current interest.

17.1.1 Ion Receptors

Aggregates such as Ca^{2+} -ionomycin, and related complexes of alkali and alkaline earth cations with polyether antibiotics, offer a natural paradigm for the recognition of alkali metals.⁷ Similarly, the complexation of Fe^{III} by siderophiles has suggested structural bases for the selective recognition of transition metal ions. Figure 1 shows some representative assemblies that recognize monoatomic and polyatomic ions.

17.1.2 Small Molecule Receptors

There are many natural paradigms for these receptor-target assemblies; the recognition of D-Ala-D-Ala vancomycin is one of the best understood, both theoretically and experimentally.³ The fundamental stimulus for this work is the need to understand the recognition of small molecules by enzymes and receptors.⁸ The recognition of other small molecules, such as barbituric acid, imidazole, and molecules of biological interest (including the amino acids and cholesterol) is being examined by many groups. This interest has, however, broadened to encompass recognition in nonaqueous solution, and to include classes of aggregates for which there are no precedents in nature. Figure 2 shows representative examples of receptors that recognize small organic molecules. The relative ease with which calixarenes, cryptands, and cyclodextrins can be synthesized has led to active communities engaged almost exclusively in their study.

17.1.3 Molecular "Machines"

The work of Stoddart and co-workers (Equation (1)) and Shanzer^{9a} and co-workers (Equation (2))^{9b} exemplifies the concept of molecular machines as primitive switches that show "off" and

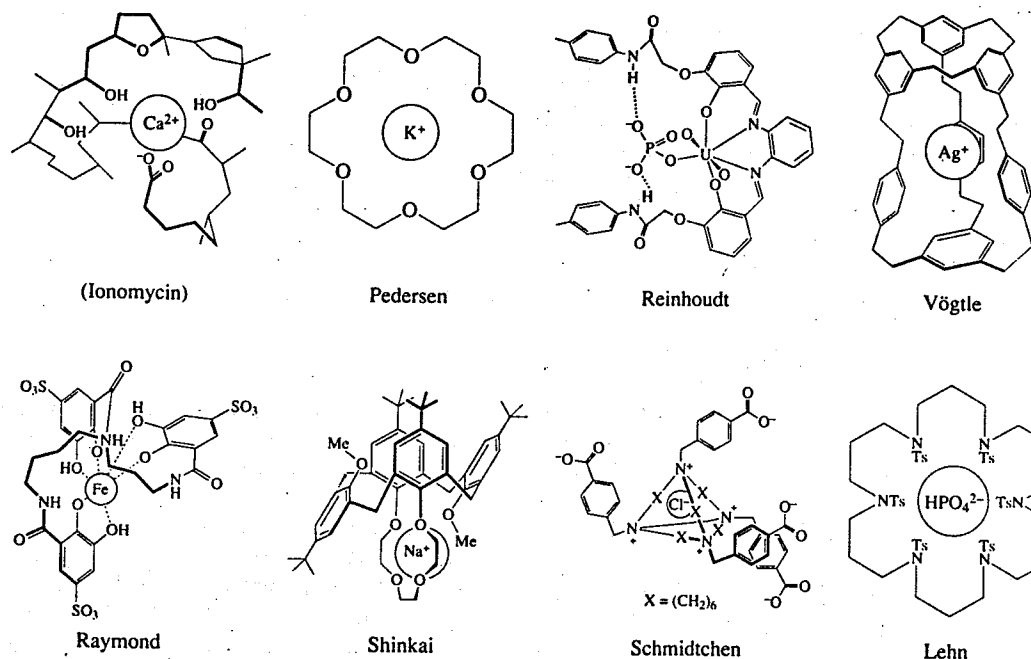
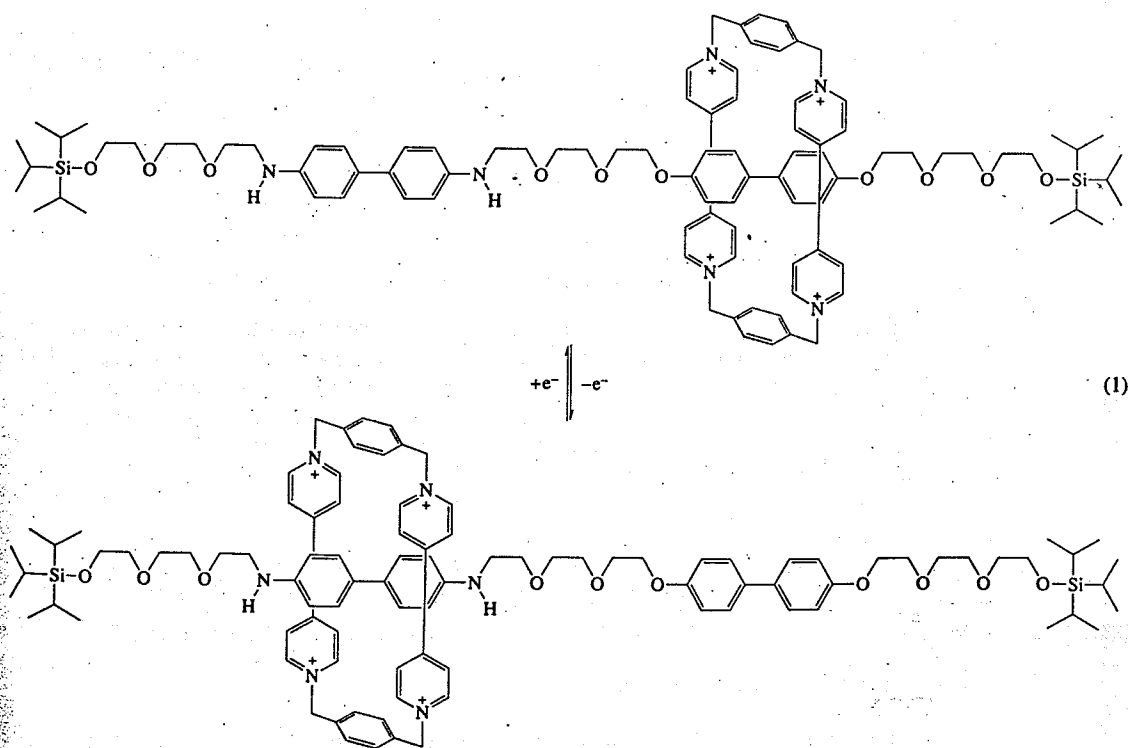


Figure 1 Recognition of ions in solution.

"on" states as a function of a physical stimulus such as redox or pH. Current molecules and aggregates are molecules that exist in different states under different conditions, but show no switching function. The gap between structure and useful function in these materials remains large, and the classes of the materials ultimately developed in this area will probably reflect the requirements for "utility" as defined by information and sensor technologies, rather than biological precedent.



materials utilizing
cyanuric acid
and crystalline

assembly of non-
covalent
derivatives,¹
D-Ala-D-Ala³
activity of these
pioneered by
numbers of

chemistry. By
interactions
ples of self-
classes have

earth cations
Similarly,
active recog-
it recognize

ation of D-
ntally.³ The
molecules by
c acid, imi-
ol) is being
ognition in
ecedents in
rganic mol-
synthesized

(Equation
"off" and

17.6.2	Motifs and Structure	616
17.6.2.1	Linear tapes: small peripheral groups	616
17.6.2.2	Crinkled tapes: medium-sized peripheral groups	618
17.6.2.3	Rosette: large peripheral groups	618
17.6.3	Implications for Crystal Engineering	618
17.6.3.1	Cocrystallization is difficult	618
17.6.3.2	Conformational complexity and polymorphism	619
17.6.3.3	The utility of powder diffraction	619
17.7	CONCLUSIONS	619
17.8	REFERENCES	620

17.1 INTRODUCTION

This chapter summarizes efforts to construct soluble aggregates and crystalline materials utilizing the noncovalent interactions (principally hydrogen bonds) between derivatives of cyanuric acid (CA) and melamine (M). The discussion is divided into two parts: soluble aggregates and crystalline materials.

Organic chemistry is turning from the synthesis of covalent molecules to the assembly of non-covalent aggregates. This shift in interest reflects both a high degree of mastery of covalent synthesis, and realization of the importance of noncovalent interactions. The dissection of natural systems—exemplified by Mrksich and Dervan's examination of *ds*DNA-distamycin derivatives,¹ Schreiber's study of FK-506-FKBP,² and Williams *et al.*'s inquiries into vancomycin-D-Ala-D-Ala³—has begun to clarify their structural and thermodynamic foundations. The specificity of these naturally occurring systems is not matched by design-based efforts of the type pioneered by Pedersen,⁴ Cram,⁵ and Lehn.⁶ These efforts have, nonetheless, produced increasing numbers of aggregates of different classes.

The design of noncovalent aggregates is now a central challenge for organic chemistry. By keeping the number of particles and/or the number of different types of noncovalent interactions to a manageable number, it is beginning to be possible to develop general principles of self-assembly. While several classes of designed assemblies have been explored, four main classes have emerged as foci for current interest.

17.1.1 Ion Receptors

Aggregates such as Ca^{2+} -ionomycin, and related complexes of alkali and alkaline earth cations with polyether antibiotics, offer a natural paradigm for the recognition of alkali metals.⁷ Similarly, the complexation of Fe^{III} by siderophiles has suggested structural bases for the selective recognition of transition metal ions. Figure 1 shows some representative assemblies that recognize monoatomic and polyatomic ions.

17.1.2 Small Molecule Receptors

There are many natural paradigms for these receptor-target assemblies; the recognition of D-Ala-D-Ala vancomycin is one of the best understood, both theoretically and experimentally.³ The fundamental stimulus for this work is the need to understand the recognition of small molecules by enzymes and receptors.⁸ The recognition of other small molecules, such as barbituric acid, imidazole, and molecules of biological interest (including the amino acids and cholesterol) is being examined by many groups. This interest has, however, broadened to encompass recognition in nonaqueous solution, and to include classes of aggregates for which there are no precedents in nature. Figure 2 shows representative examples of receptors that recognize small organic molecules. The relative ease with which calixarenes, cryptands, and cyclodextrins can be synthesized has led to active communities engaged almost exclusively in their study.

17.1.3 Molecular "Machines"

The work of Stoddart and co-workers (Equation (1)) and Shanzer^{9a} and co-workers (Equation (2))^{9b} exemplifies the concept of molecular machines as primitive switches that show "off" and

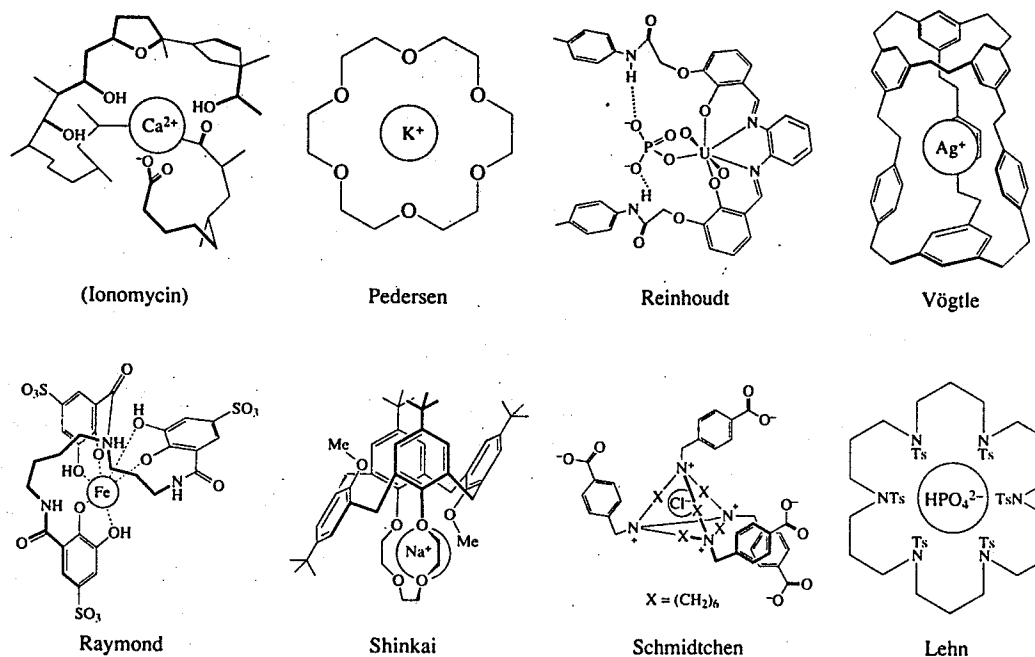
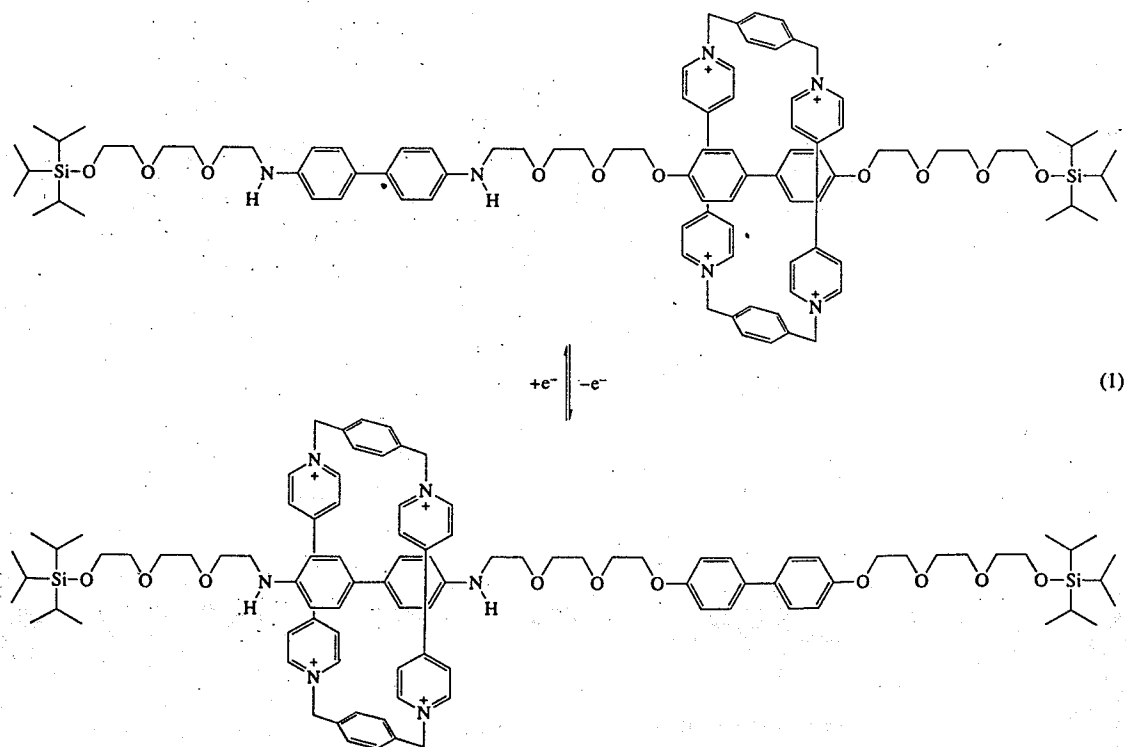
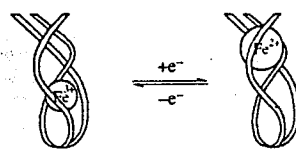


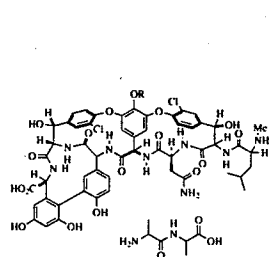
Figure 1 Recognition of ions in solution.

"on" states as a function of a physical stimulus such as redox or pH. Current molecules and aggregates are molecules that exist in different states under different conditions, but show no switching function. The gap between structure and useful function in these materials remains large, and the classes of the materials ultimately developed in this area will probably reflect the requirements for "utility" as defined by information and sensor technologies, rather than biological precedent.

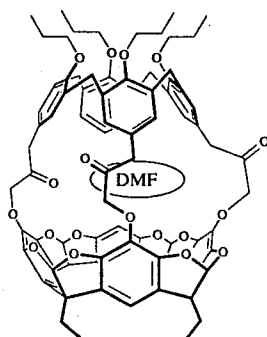




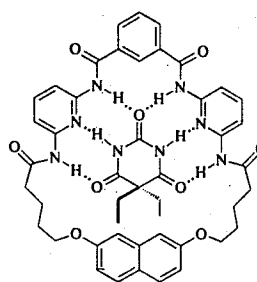
(2)



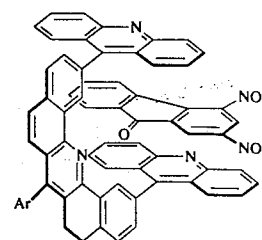
(Vancomycin)



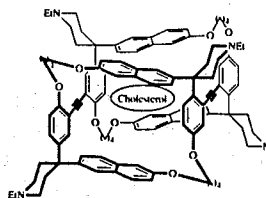
Reinhoudt



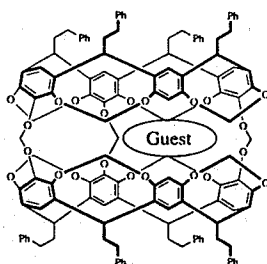
Hamilton



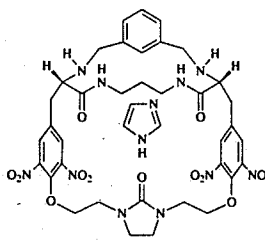
Zimmerman



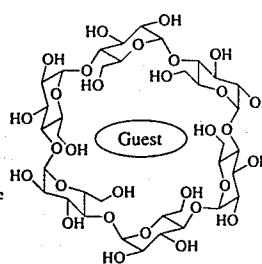
Diederich



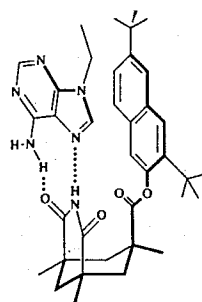
Cram



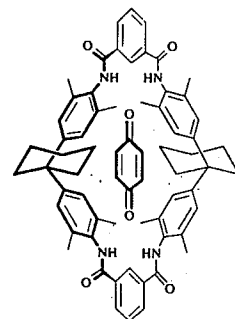
Still



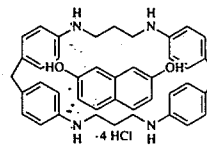
Breslow



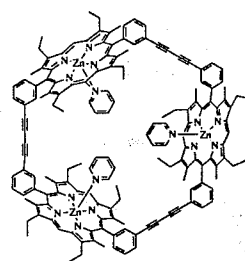
Rebek



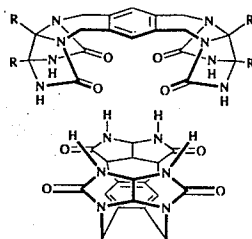
Hunter



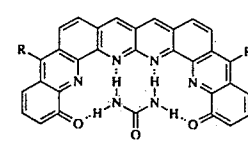
Koga



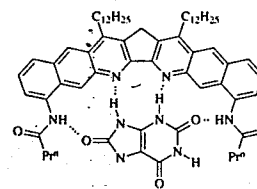
Sanders



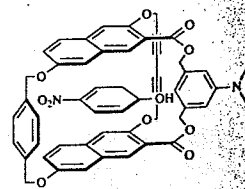
de Mendoza and Rebek



Bell



Kelly



Whitlock

Figure 2 The recognition of small molecules.

171.4 Multiparticle Aggregates

Many important recognition events involve multiple particles (either connected or independent): formation of molecular crystals; folding of proteins; assembly of multiprotein structures such as ribosomes and viral capsids; formation of lipid bilayers and liposomes.¹⁰ These large assemblies can serve as structural elements in materials and catalysts, and as molecular scaffolds that orient and position functional components. tRNA is one example of a molecular scaffold: holding recognition and reaction domains at a specific distance in specific orientations is accomplished by a combination of hydrogen bonding and other interactions present on an oligonucleotide backbone. Enzymes provide another sophisticated example in which many recognition and catalytic elements are positioned by a self-assembled structure. Figure 3 shows examples of synthetic scaffolds.

17.2 OUR WORK

Our own efforts in noncovalent synthesis and molecular self-assembly center on the construction of multiparticle aggregates. We have used derivatives of CA and M to investigate self-assembly both in solution and the solid state. (We refer to any derivative of isocyanuric acid or barbituric acid as CA.) The system offers, as one of its assets, a strong conceptual complementarity between soluble aggregates and crystalline solids. While the majority of this chapter is dedicated to the description of soluble aggregates, efforts in the solid state have suggested important concepts—especially those based on steric constraints to shape (peripheral crowding)—that are also directly applicable in soluble assemblies.

17.3 CA·M

The CA·M lattice is shown in Figure 4. We have identified three different motifs that are useful as scaffolds for the construction of soluble aggregates and crystalline materials: the rosette, and the linear and crinkled tapes. The construction of soluble scaffolds requires a simple, soluble, and discrete system: our efforts focus on the rosette. The study of crystalline materials benefits by

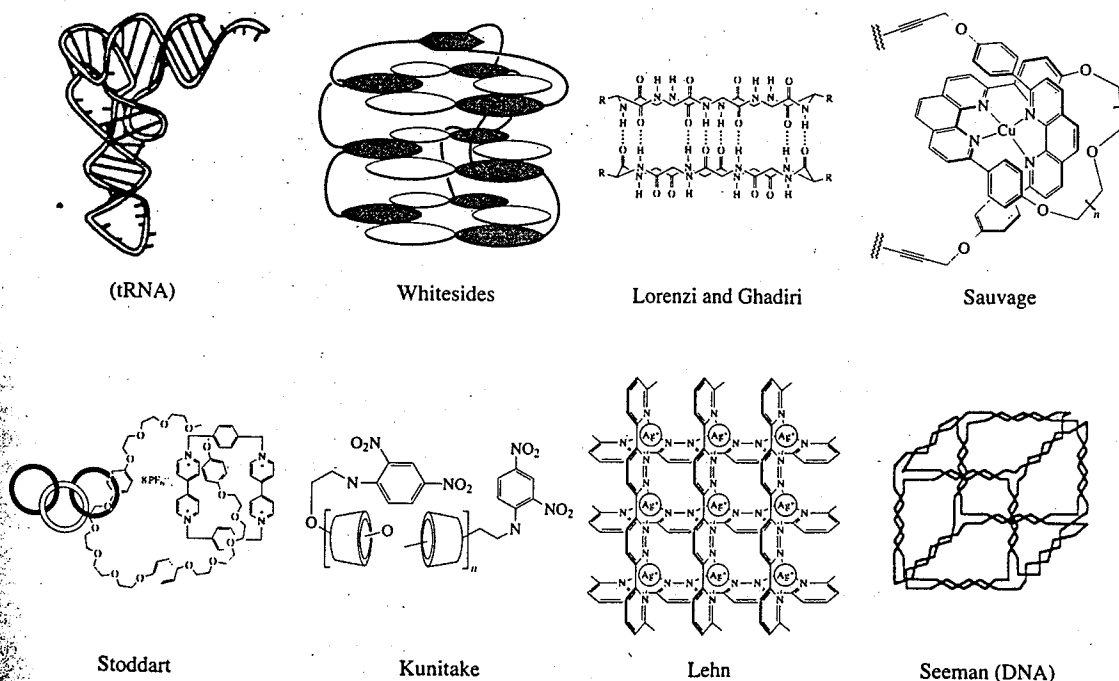


Figure 3 Scaffolds based on noncovalent interactions.

reducing the dimensionality of the problem: learning the rules governing the alignment of quasi-one-dimensional tapes in the solid state should be easier than understanding the packing of "zero-dimensional" molecules with no constraints on their orientation. The solubility of extended tape structures is low and they are, for that reason, good choices for work with solids, but poor choices for soluble systems.

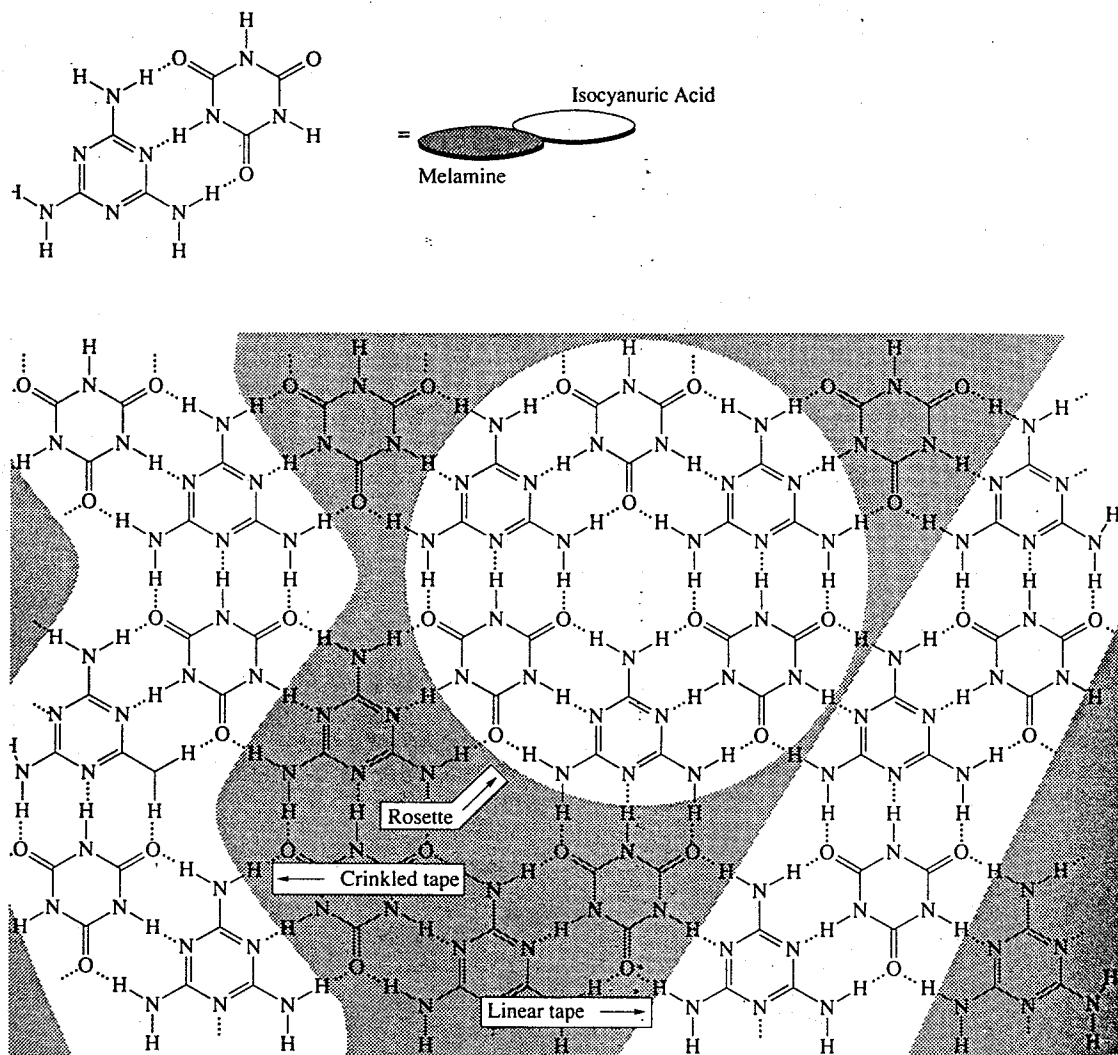


Figure 4 The lattice of isocyanuric acid and melamine. Three motifs are highlighted: two extended tape motifs and the discrete rosette. We represent melamines as darkened disks and isocyanuric acids as white

In addition to affording motifs for the design and construction of soluble aggregates or crystalline solids, CA-M offers additional advantages: the relatively high stability reflects the network of hydrogen bonds between molecules of CA and M; the ease of characterization due to the symmetries of the individual molecules and resulting assemblies; the straightforward synthesis of derivatives of CA and M. We comment on each of these advantages separately.

17.3.1 Hydrogen Bonds

The assembly of an aggregate in solution requires that the enthalpic gain resulting from the formation of new bonds exceeds the entropic costs of bringing molecules together. The enthalpy of aggregation can be influenced in two ways: by increasing the strength of the interaction (van der Waals forces < hydrogen bonds < metal chelates < covalent bonds), and by increasing the

number of bonds being formed. The assembly of a multiparticle aggregate must occur reversibly if it is to lead to a structurally well-defined system. The importance of reversibility stems from the fact that irreversible association of components in solution will usually result in a number of different aggregates, and kinetic assembly will not normally cleanly generate the most thermodynamically stable aggregate. For the target (equilibrium) structure to form, the components of the assembly must be able to reorganize repeatedly and with small expense in energy: if the enthalpy of the interactions is too high, the favored product can be made kinetically inaccessible.

We (and many others) choose to use hydrogen bonds for our studies of noncovalent assembly. Each hydrogen bond in a structure based on the CA-M lattice contributes $4.186\text{--}12.56\text{ kJ mol}^{-1}$ to the enthalpy of aggregation in chloroform solution. This value is comparable to $RT = 2.51\text{ kJ mol}^{-1}$ at 300 K, and equilibrium among aggregates is usually rapid. Although this value is relatively small compared to charge-charge interactions in nonpolar solvents, and to some metal-chelate interactions, the total enthalpy of aggregation can be "tuned" by increasing or decreasing the total number of hydrogen bonds. Hydrogen bonds offer additional advantages: they involve distinct donor and acceptor groups, and they are directional: they thus offer more possibility for structural design than forces that are symmetric and nondirectional.¹¹

17.3.2 Symmetries

Molecules of CA and M are effectively C_2 symmetric with respect to the axis connecting the two sets of interacting hydrogen bonds. Functionalizing the third edge of a CA usually does not influence this symmetry. Functionalizing molecules of M can decrease this symmetry: it introduces a potential for isomerism in some of these aggregates (Figure 5). While this isomerism can complicate structural characterization, it can also provide important information about the rigidity of the framework that organizes the hydrogen-bonded components. Isomerism due to the linker groups on M does not change the positions at which CA is recognized, that is, isomerism does not affect shape, and therefore, probably does not affect function. We discuss isomerism in more detail in Section 17.5.2.8.

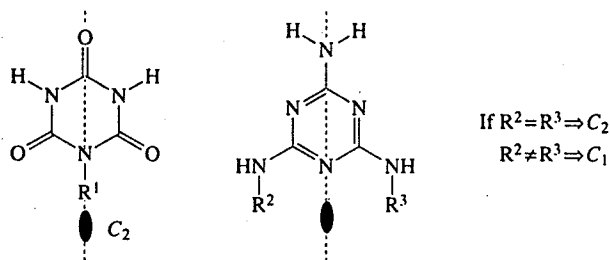


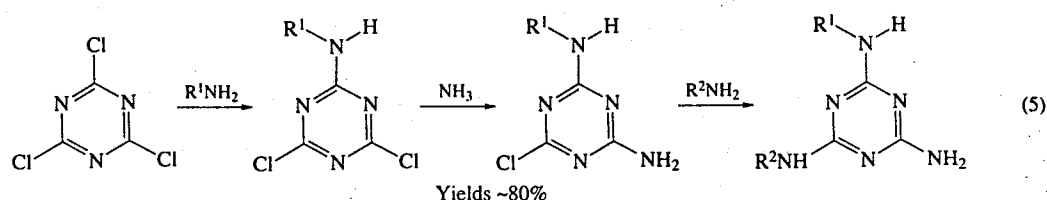
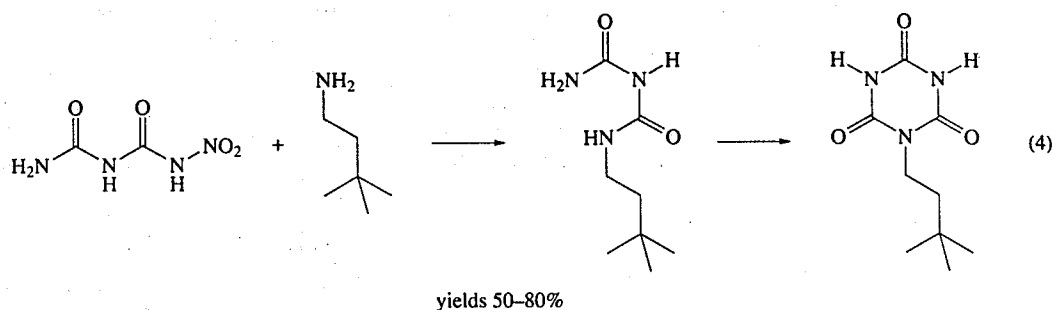
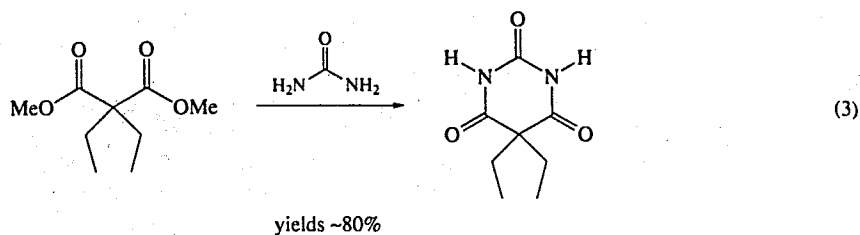
Figure 5 CA are C_2 symmetric unless R^1 is chiral. For M, unless $R^2 = R^3$, there is no C_2 symmetry.

17.3.3 Synthesis

The synthesis of the linker groups used for tethering melamines or cyanuric acids is not difficult; details are available in the original sources.¹² The efficient generation of derivatives of CA and M is also relatively straightforward, but is sufficiently challenging that it deserves some comment. The methods used for the "synthesis" of the noncovalent aggregates that form when derivatives of CA and M are mixed also requires description.

Two types of molecules related to CA are used in these studies. Diethylbarbital (and other derivatives of barbituric acid) come from the condensation product of diethyl dialkylmalonate and urea (Equation (3)). Neohexylisocyanuric acid and other *N*-substituted derivatives of CA are synthesized in two steps from the appropriate amine (Equation (4)). Reaction of an alkylamine with nitrobiuret yields an isolable intermediate—an alkylbiuret—which is cyclized with a carbonyl source such as diethyl carbonate and carbonyl diimidazole. Yields are often high (60%), but depend strongly on the amine used. Many derivatives of CA are commercially available.

Cyanuric chloride reacts selectively with amines and generates trisubstituted melamines (Equation (5)). The first equivalent of amine (typically an unreactive aniline derivative) is added at 0°C . After 10 min, a second amine (such as NH_3) is added. After stirring at room temperature for 90 min, the final amine (often a reactive alkyl or benzyl amine) is added. Refluxing these reactants for 8 h yields the trisubstituted melamine in $\sim 80\%$ yield.



The ease of synthesis of an aggregate from its components depends partially on their solubility in chloroform: most molecules of CA are only slightly soluble in organic solvents. When both components are soluble, simply mixing them generates the aggregate. Heating the components at reflux in chloroform for ~30 s yields aggregates for all but those containing the least soluble components. In these final cases (i.e., the bis(rosette) that will be introduced later), approximately 5% methanol is added to the chloroform to increase solubility, and the mixture of components is refluxed. The solution is evaporated to dryness. The observation that the resulting powder is completely soluble in chloroform is an indication that aggregation is occurring.

17.4 ORGANIZATION OF THIS CHAPTER

For simplicity, we divide this review into two sections—soluble aggregates and crystalline tapes. We discuss similarities between these systems as they arise.

17.5 SOLUBLE AGGREGATES

We divide our discussion of soluble aggregates (shown pictorially in Figure 6) into four parts. Design describes two strategies for noncovalent synthesis: preorganization and peripheral crowding. Characterization outlines the methods we employ to assign structure; evaluating isomerism is discussed in this section. Computation summarizes our initial efforts to rationalize the relative stabilities of a series of simple aggregates. Theory sketches our efforts to arrive at a conceptual framework and structure-based parameters for comparing stabilities of aggregates, in order to make it possible to design new structures.

17.5.1 Design

We have applied two strategies to the design of noncovalent assemblies based on the CA-M lattice: preorganization and peripheral crowding. Cram's rule of preorganization qualitatively highlights the entropic aspects of self-assembly.¹³ The rule states that the assembly occurring with

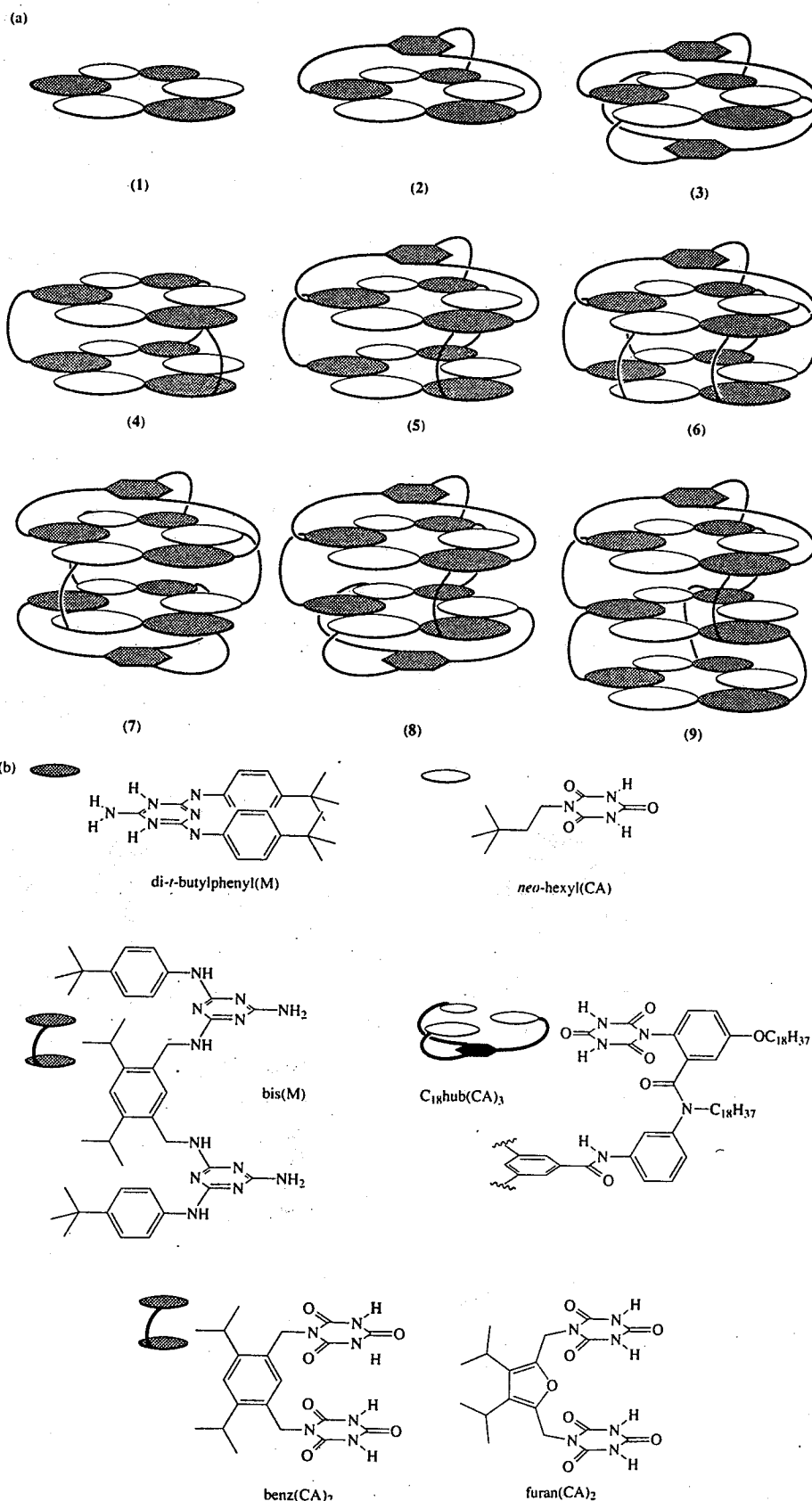


Figure 6 (a) Nine structurally similar classes of aggregates have been explored. All are based on the rosette motif; atomic detail is provided in (b) and (c) (source: Whitesides *et al.*¹⁰).

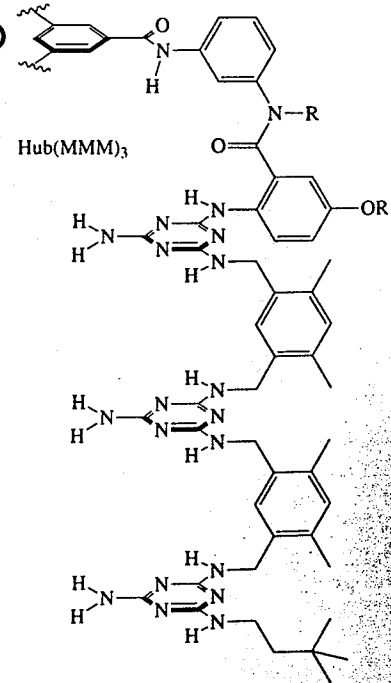
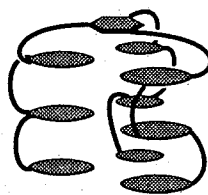
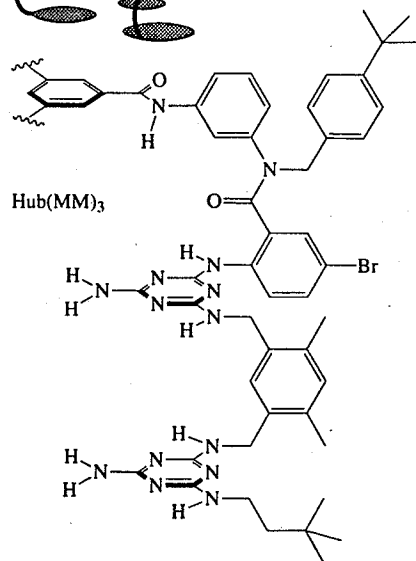
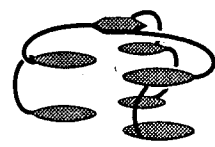
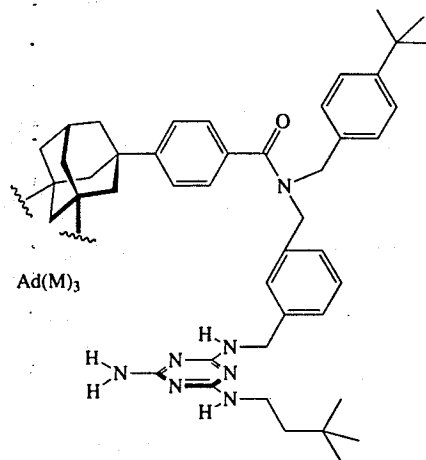
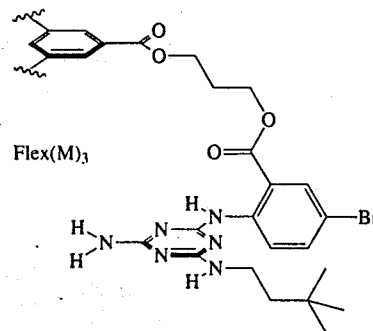
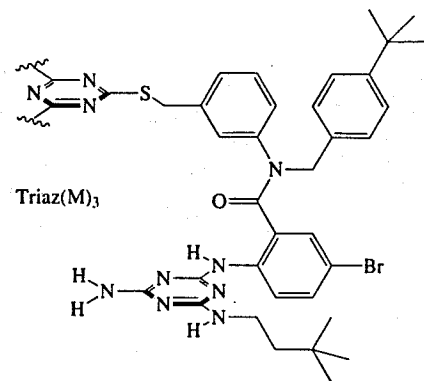
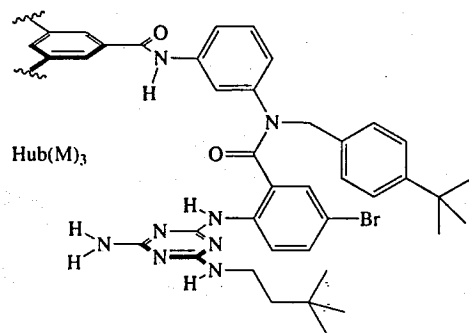

$$R = C_{18}H_{37}$$

Figure 6 (continued)

the smallest loss of entropy is most favorable. Preorganization is most efficiently discussed in terms of the entropies affected: translational, rotational, and conformational. Peripheral crowding describes a strategy for design that favors one recognition motif over a second by designing enthalpic costs into the two through steric overlaps. This strategy is related, conceptually, to the use of the *gauche* effect in influencing conformational equilibria in covalent organic molecules.

17.5.1.1 The effect of preorganization on the translational entropy (ΔS_{trans}) of assembly

If N particles assemble, the magnitude of ΔS_{trans} is proportional to $N-1$ (Equation (6)).¹⁴

$$\Delta S_{trans} = (N-1) \left[\frac{5}{2}R + R \ln \frac{V}{N} \left(\frac{2\pi kT}{h^2} \right)^{3/2} \left(\frac{M_p}{M_{ass}} \right)^{3/2} \right] = (N-1)C_{trans} \quad (6)$$

We expect (and observe experimentally) that (1), comprising 6 molecules joined by 18 hydrogen bonds, will be less stable than (3), comprising 2 molecules joined by 18 hydrogen bonds. Linking the recognition domains (such as M in $\text{hub}(\text{M})_3$ and CA in $\text{hub}(\text{CA})_3$) by tethers—and thereby reducing ΔS_{trans} —has yielded a series of stable aggregates (Figure 6(a)).

17.5.1.2 The effect of preorganization on rotational entropy (ΔS_{rot})

The entropic cost associated with loss of rotational entropy on assembly, like that of translational entropy, is proportional to the number of particles (Equation (7)).¹⁴ Reducing the number of particles will also reduce the magnitude of the entropic cost of aggregation.

$$\Delta S_{rot} = (N-1) \left[R \ln \left(\frac{8\pi^2 ekT}{h^2} \right) \left(\frac{I_p}{I_{ass}} \right) \right] = (N-1)C_{rot} \quad (7)$$

17.5.1.3 The effect of preorganization on conformational entropy (ΔS_{conf})

Most of our efforts are invested in understanding and minimizing the costs of the reduction of conformational entropy on assembly. These costs come from requiring freely rotating single bonds to adopt a single conformation (or a limited set of conformations) upon aggregation. Ideally, we want the geometries of the preassembled components to be similar to those adopted in the aggregate. $\text{Hub}(\text{M})_3 \cdot 3\text{neo-hexyl}(\text{CA})$, (2)—the model system for most of the aggregates generated to date—incorporates attempts that we envision to lead to preorganization: rigid linking groups; curved tethering arms.

The majority of bonds in $\text{hub}(\text{M})_3$ are rigid: aromatic rings and amides. By contrast, $\text{flex}(\text{M})_3$ contains polymethylene chains linked by esters. We have not quantitatively explored the relative stabilities of aggregates derived from these compounds; stability correlates qualitatively with rigidity. We comment on this correlation further in Section 17.5.3.

All of the tethered molecules were designed to place the recognition element in the appropriate orientation. Much of this positioning is accomplished by the substitution of aromatic groups. We hypothesized that *m*-phenylenediamine and *o*-anthranilate of $\text{hub}(\text{M})_3$ might cooperate in forming a 180° turn that oriented the melamine groups beneath the central core, that is, into a geometry that allows them to form networks of hydrogen bonds with molecules of CA. We believe that the *m*-xylenyl linker of $\text{hub}(\text{MM})_3$ (of (5)) offers the same type of preorganization.

17.5.1.4 Peripheral crowding

Peripheral crowding is a strategy for favoring a mono- or bis(rosette) (1) or (4) in solution rather than a tape by increasing the size of the groups on the periphery (Figure 7). Unfavorable steric interactions between these substituents maximize the distance between them; this distance increases as the three motifs are ordered: linear tape < crinkled tape < rosette. Tables 1 and 2 show the dependence of stability of bis(rosettes) on the size of the peripheral groups.

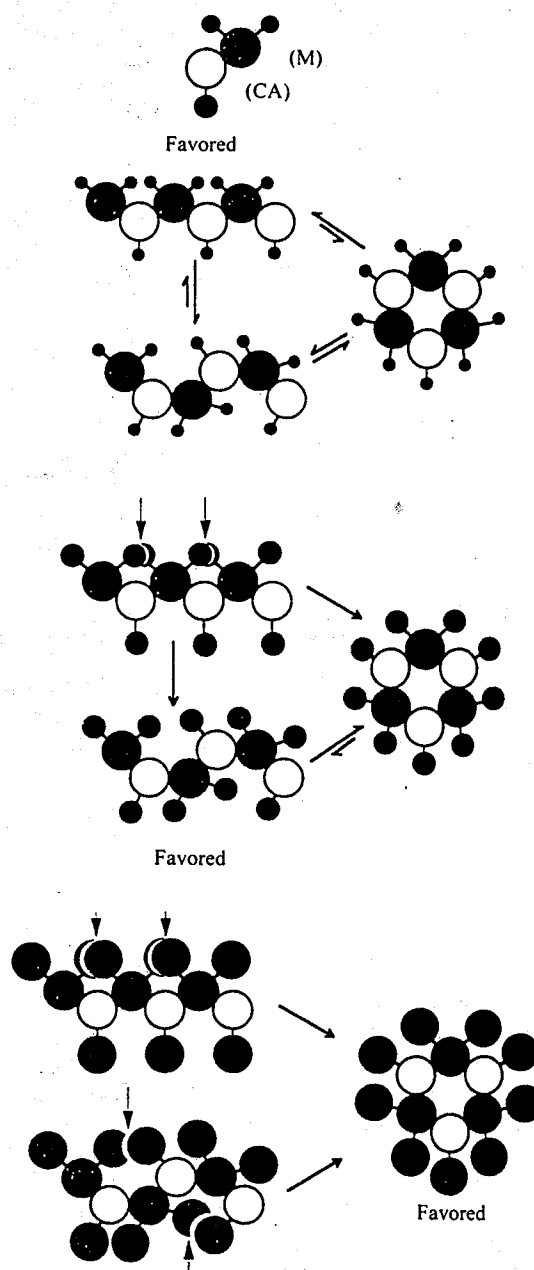
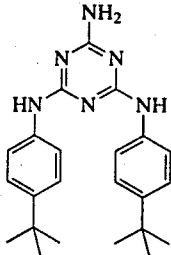
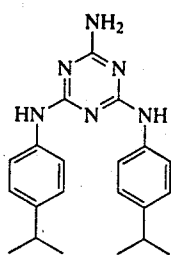
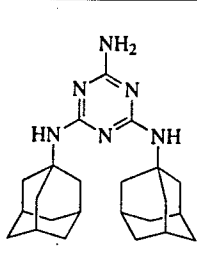
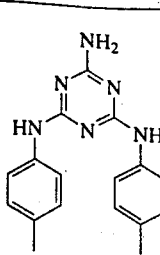
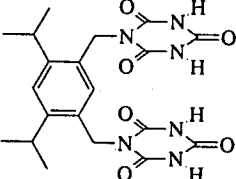
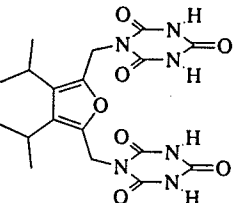


Figure 7 Peripheral crowding describes the preference for the indicated motif based on the size of the peripheral groups (pg: indicated as blackened disks). When the pg are small, we observe linear tapes in the solid state. As pg get larger, steric overlap (arrows) between them result in the formation of crinkled tapes over linear tapes. Rosettes are favored over both tape motifs when the pg become large.

17.5.2 Characterization

We assign structures to soluble aggregates based on the summation of inferences from a number of techniques; no single technique is completely convincing in these systems, and we have not, with one exception, been able to obtain diffraction-quality crystals for x-ray structure analysis.¹⁵ Experiments that use NMR spectroscopy to follow the titration of the M component by addition of CA have established the relative stoichiometries of components; differences in solubility between aggregates and individual molecules of CA and M are a useful indicator of aggregation. Molecular weights can be determined by vapor phase osmometry (VPO), electrospray-ionization mass spectrometry (ESI-MS), and gel permeation chromatography (GPC). The shape of the GPC

Table 1 Increasing the size of the peripheral groups favors rosette formation. Aggregates which are stable indefinitely are marked with (++). Unsuccessful formation of an aggregate is indicated with (-).

				
	++	-	-	-
	++	-	-	-

trace and methanol titrations provide another type of estimate of the stabilities of these aggregates. The majority of detail about structure (number and symmetries of isomers) comes from ^1H NMR spectroscopy; ^{13}C NMR spectroscopy is also useful.

17.5.2.1 Stoichiometry

Proton-NMR spectroscopy can be used to monitor titration experiments that yield the ratio of CA:M. Visual inspection corroborates the result. To a solution of the soluble M component, the CA component (which is insoluble by itself) is added. Assembly is cooperative in most cases—sharp lines (those of the final aggregate) appear superimposed on the broadened spectrum of the melamine; there is no spectroscopic evidence for intermediate complexes with different stoichiometries. The intensities of the lines increase until some integral stoichiometry is reached (for (2), lines increase in intensity until three equivalents of CA have been added); beyond this point, CA is no longer soluble and a suspension of insoluble material can be observed.

17.5.2.2 The determination of molecular weight: vapor phase osmometry

Molecular weights can be estimated using VPO—a technique based on the difference in vapor pressures of a pure solvent and solutions containing aggregates. Known amounts of aggregate (or standard) are dissolved in chloroform and applied in small volumes (300 μL) to a thermistor. Pure chloroform is applied to a second thermistor. The two thermistors are kept at the same temperature by passing current through heating elements; the voltage is monitored. This voltage is recorded for a series of concentrations (5–100 mM), and the values are extrapolated to infinite dilution. The results are compared to values obtained using standards of known values of MW. The result is a number-averaged MW. The value for MW is typically accurate to within only 20% of the expected value, and depends strongly on the standard used as a reference of MW. Many standards are used in an effort to check for (and control) the nonidealities of the system.

Table 2 Increasing the size of the peripheral groups favors rosette formation. Aggregates which are stable indefinitely are marked with (++). Aggregates that formed, but were stable in solution for days, are marked with (+). Unsuccessful formation of an aggregate is indicated with (-).

Increasing steric bulk of R ²					
R ² = H R ¹ = Pr ⁱ	++	++	-	-	
R ² = Bu ^t R ¹ = Pr ⁱ	++	++	++	+	
Increasing preorganization (size of R ¹)					
R ² = Bu ^t R ¹ = Me	++	+	-	-	
R ² = Bu ^t R ¹ = H	+	+	-	-	
R ² = Me R ¹ = H	+	-	-	-	

17.5.2.3 The determination of molecular weight: gel permeation chromatography

GPC is a size exclusion technique. Solutions of aggregates are injected onto a column containing semiporous polystyrene beads having a narrow distribution of pore sizes. Molecules (or aggregates) small enough to diffuse into the stationary liquid in the pores move through the column more slowly than larger molecules that are sterically excluded from the pores. Figure 8 shows the correlation between retention time and molecular weight (which correlates with size). The trend observed with the aggregates is similar to that seen with soluble polystyrene, although the slopes of the lines are significantly different. We show two dashed lines on the graph corresponding to aggregates comprising one and two rosettes. While the difference between these lines suggest that it may ultimately, with greater understanding of GPC, be possible to distinguish between these and other structural motifs for CA-M-based aggregates based on their shape, it is not currently possible to draw conclusions (based on the limited numbers of aggregates explored) beyond molecular weight. Even in this limited sphere, GPC is not useful in estimating molecular weight unless compounds that are structurally closely related are being compared. We use GPC primarily to estimate relative stabilities of aggregates (see below), rather than their molecular weights.

17.5.2.4 The determination of molecular weight: electrospray ionization mass spectrometry

Molecular ions corresponding to the assembled aggregates associated with one or more equivalents of Cl⁻ have been recorded using ESI-MS for many of our more stable aggregates. Ionization is accomplished from solutions of the aggregate in chloroform containing Ph₄P⁺Cl⁻ as a soluble source of Cl⁻.¹⁶ In general, the values of MW obtained from ESI-MS are those expected for the hypothesized structure.

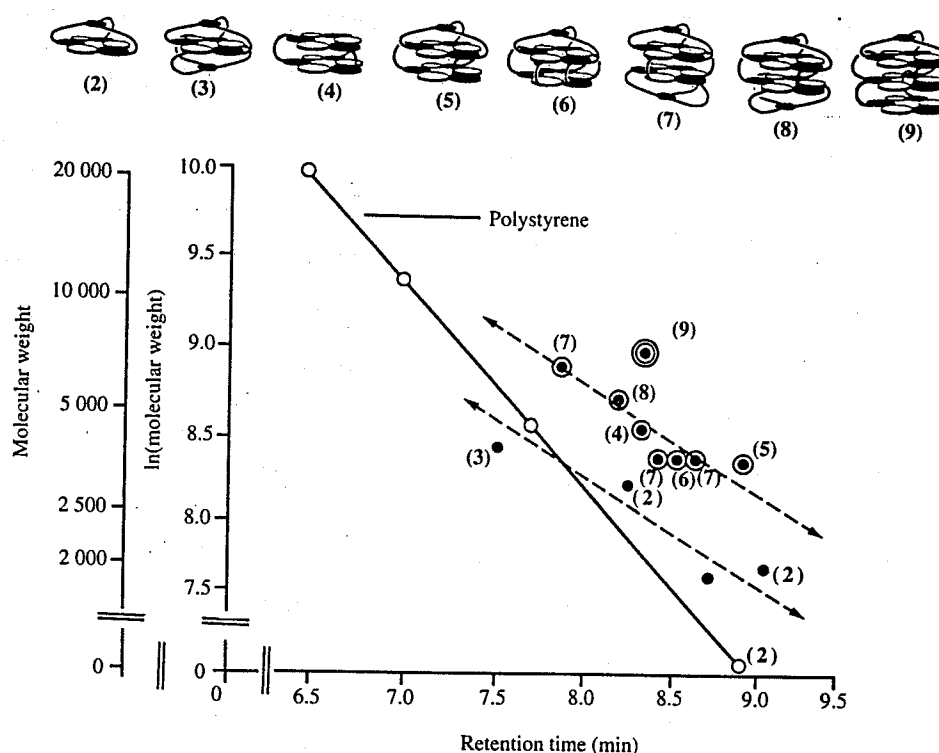


Figure 8 The retention time from gel permeation chromatograms of (2)–(9) correlate with molecular weight. The dotted lines organize similar classes of aggregates: those comprising single rosettes (solid dot) are distributed around the lower line; aggregates comprising two rosettes (ringed dot) are distributed around the higher line. Aggregate (9) (with three rosettes) is shown with a double-ring dot. Both lines appear to have similar slopes, suggesting a similar shape-dependent behavior.

Table 3 compares the MW determined by a variety of techniques. While ESI-MS is by far the most accurate, GPC and VPO still offer interesting and useful information about stabilities and nonideal behaviors.




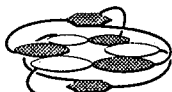
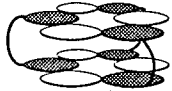


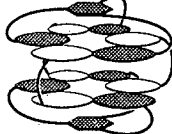
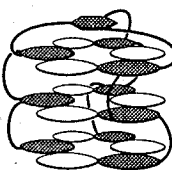
17.5.2.5 Relative stability: methanol titrations

One of the aggregates based on CA·M (1) must be at concentrations above 4 mM to be observable by NMR spectroscopy—at concentrations below 4 mM, the NMR spectrum appears as a superposition of the spectra of the individual components. The remaining aggregates exhibit concentration-independent stability: they are observable by NMR spectroscopy up to dilutions (< 0.05 mM) at which covalent molecules are not observed. The relative stability of these aggregates can be determined by measuring the lifetime of the aggregate in solutions containing methanol- d_4 .¹⁷ The most stable aggregate slowly dissociates over 3 d in 20% methanol (v:v): ~5 M CD_3OD in 10 M $CDCl_3$. The remaining aggregates can be ordered by their lifetime in solutions containing 5% or 10% methanol in chloroform. The results of this ranking are shown in Table 4 and will be discussed in greater detail later.

17.5.2.6 Relative stability: analysis of the GPC trace

The extent of tailing of the GPC trace yields information about the stability of the aggregate. We consider any aggregate that elutes from the column to be stable; aggregates that dissociate and precipitate on the column are unstable. Figure 9 shows the GPC traces of representative aggregates. Of the aggregates that elute, we believe that the extent of tailing of the GPC trace correlates with the stability of the aggregate: more stable aggregates elute as sharp peaks; less stable aggregates tail. Tailing results when the partial dissociation of CA molecules provides a soluble aggregate of slightly different shape and mass than the original aggregate (and often, a longer elution

Table 3 Calculated and experimental molecular weights for a series of aggregates.

Aggregate		Calculated	ESI-MS	VPO
	(1)	1724.2	a	1700
	(2a)	2732.7	2732.7	3200
	(2b)	1961.2	3922.6 ^b	4000
	(3)	4100.6	4100.2	6500
	(4)	3635.5	a	3700
	(5)	4142.6	4142.6	4200
	(6)	4196.4	4196.1	4500
	(7)	5519.5	5519.1	5400
	(9)	6440.6	6433.8	6500

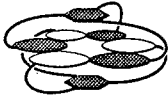
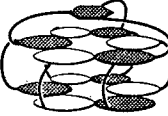
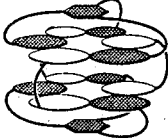
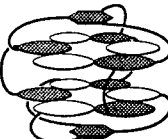

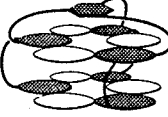
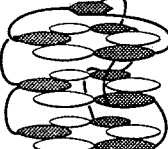

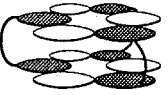

^aMolecular ions were not observed for these aggregates. ^bNo molecular ion corresponding to the hypothesized structure was observed, only an ion corresponding to the dimer.

time). If the dissociation of components yields insoluble by-products (dissociation triggers complete and irreversible dissociation and precipitation of all components onto the matrix), the eluting peak may appear uncharacteristically sharp. The unexpected sharpness of (4) may result from this situation: both components are insoluble in chloroform, unless organized into a bis(rosette).

17.5.2.7 ¹H and ¹³C NMR spectroscopies

NMR spectroscopies have yielded the majority of structural information about these aggregates. The ¹H and ¹³C NMR spectra of unassociated components—especially the polymelamines—show very broad peaks due to nonspecific aggregation. Few lines are visible in the ¹³C NMR

Table 4 Aggregates (1)–(9) are arranged in order of decreasing stability based on the percentage of methanol at which the aggregate survives. HB is the number of hydrogen bonds. *N* is the number of particles.

VPO		Percentage	HB/(<i>N</i> -1)	HB	<i>N</i>
1700		20(3)	18	18	2
3200					
4000		20	12	36	4
6500		20	9	36	5
3700					
4200		10	9	36	5
4500		5	6	18	4
5400		5	6	36	7
6500		5	6	54	10
		< 5	4	18	6
		< 5	4.5	36	6
		0	3.8	18	6

↑
Stability increases

spectra. Upon formation of the aggregate, sharp lines appear (Figure 10) in the ^1H NMR spectrum. Lines due to the N—H protons of the CA groups also appear at $\delta 16$ –13; this spectral region contains no other signals, and the pattern of lines for the N—H protons are highly diagnostic for the number of aggregates present in solution, and the symmetries of these aggregates.

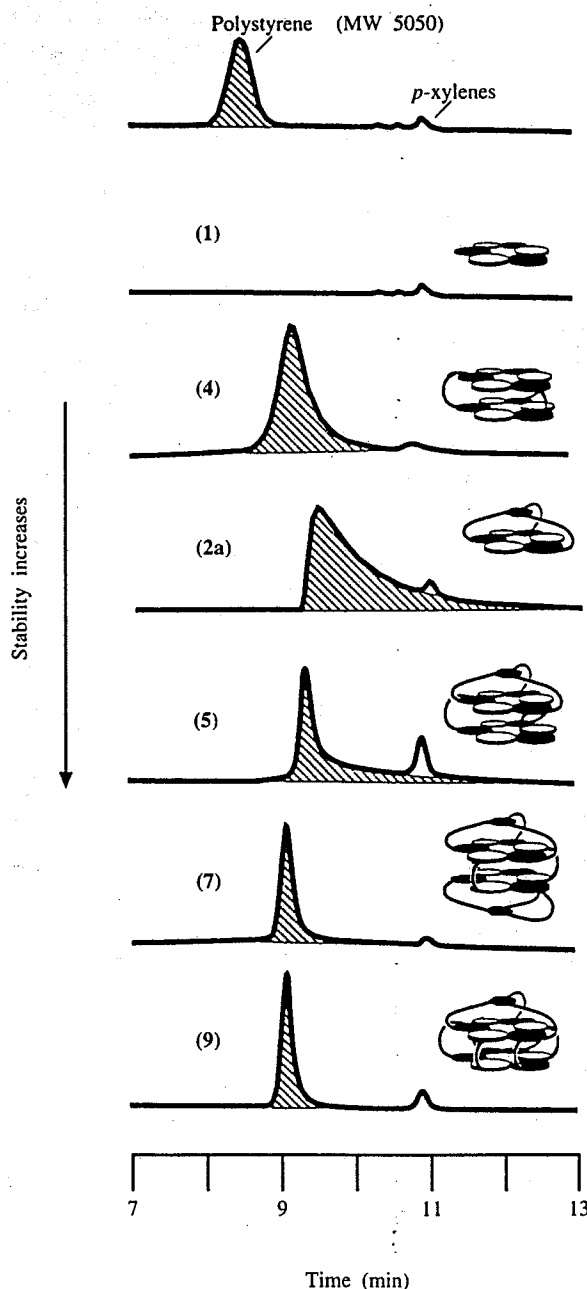


Figure 9 GPC traces for selected aggregates arranged in order of increasing stability of the aggregate.

17.5.2.8 Isomerism

As aggregates get larger, conformational isomers become more important. The NMR spectra also become increasingly complex, and the $\delta 10-0$ region almost impossible to interpret. While we envisage (and observe) only two isomers of $\text{hub}(\text{M})_3\cdot 3\text{CA}$, a structure based on a monorosette, structures based on bis(rosettes), such as $\text{hub}(\text{MM})_3\cdot 6\text{CA}$, can exist as 16 isomers. Understanding these ^1H NMR spectra and correlating their characteristics with conformational isomers of the rossettes provides a powerful method for analyzing the structures of these aggregates.

The region of the ^1H NMR spectrum at $\delta 16-13$ is diagnostic for the number of isomers, and symmetries of the isomers of $\text{hub}(\text{M})_3\cdot 3\text{CA}$.¹⁸ The hydrogen-bonded imide ($\text{N}-\text{H}\cdots\text{O}$) groups appear in this region. The symmetric isomer shows two lines as a result of the unsymmetric substitution of the adjacent melamine group. The asymmetric isomer shows six lines (Figure 11). Ratios of isomers depend on the structure of the CA used, but are not significantly influenced by

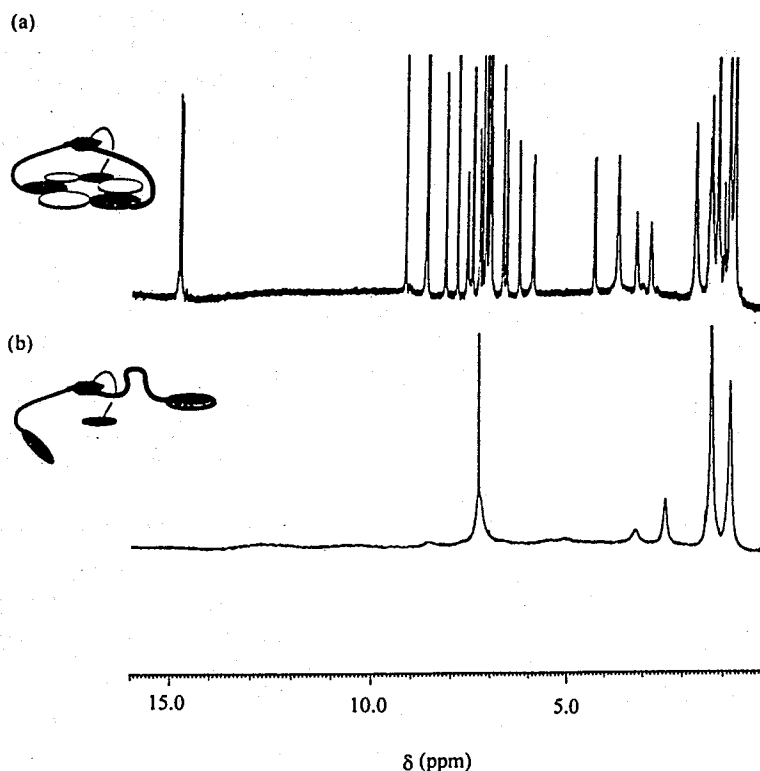


Figure 10 The ^{15}N NMR spectrum of (a) $\text{hub}(\text{M})_3 \cdot 3\text{CA}$ and (b) $\text{hub}(\text{M})_3$. The imide region ($\delta 16\text{--}13$) is uncrowded and diagnostic for the number and symmetries of aggregates present. For a complete assignment of peaks, see Simanek *et al.*¹⁸

solvent. The energy barrier to interconversion of these isomers at 328 K is $\sim 58.6 \text{ kJ mol}^{-1}$. This value is similar to the barrier of exchange of CA molecules between different pairs of adjacent melamine groups.

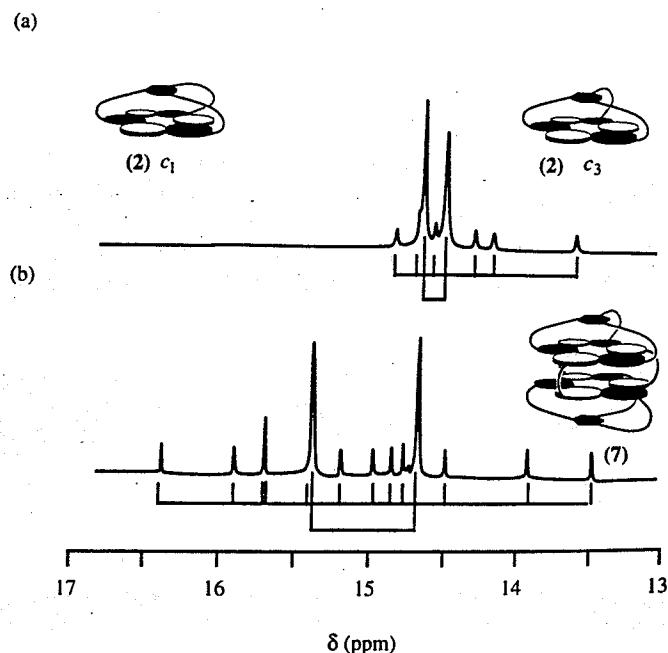


Figure 11 The imide regions of two aggregates reveals the number and symmetries of the isomers. Each spectrum shows two different aggregates. Assignment of (a) is straightforward—only two isomers exist. Assignment of (b) is less straightforward—12 isomers can exist.

More complicated aggregates behave similarly. The aggregate $2 \text{ hub(M)}_3 \cdot 3 \text{ bis(CA)}$ shows either two or five isomers, depending on the derivative of bis(CA) that is used: at least 12 isomers are theoretically possible for this aggregate. The spectra of (2) and (7) are shown in Figure 11. We do not currently understand why we observe only two isomers with benz(CA)_2 and at least five with furan(CA)_2 . The fact that isomers are observed, however, provides additional information for the assignment of structure.

17.5.3 Computation

Utilizing $\text{hub(M)}_3 \cdot 3\text{CA}$ and related structures, we have explored the use of computational models¹⁹ for determining relative stabilities. Estimating relative entropies and enthalpies for these structures computationally is not currently practical, because these calculations would require enormous amounts of time. Ideally, the method for estimating the values of entropy and enthalpy—or arriving at some stability factor that can be used to compare two aggregates—should be accessible to members of the experimental community, fast, and general enough to be applied to a large number of related structures. The role of solvent must be considered in many cases.

17.5.3.1 Starting point for the calculations and minimization strategy

The rosette was constructed by placing three M and three CA rings on a common plane in a rosette at a distance of 180 pm (measured from the N—H to Q of any hydrogen bond donor-acceptor pair). The spokes were attached to preserve the C_3 symmetry observed in the $^1\text{H NMR}$ spectrum. All torsional angles were rotated to preserve this symmetry and to maximize the distance between the rosette and central hub. Energetically unfavorable interactions were minimized by a 1000 step conjugate gradient energy-minimizing algorithm. Additional details are available in the original source.¹⁹ From this starting point, minimizations (described above) could be carried out for any of the aggregates with a structure shown by (2).

We have explored a surrogate for these values—a value that we refer to as “DP” (distortion from planarity). To calculate DP, we determine the minimized structures of aggregates built using valence geometries from QUANTA 3.3 using the CHARMM 22 force field. (The role of solvent in these calculations is discussed in Section 17.5.3.2) A plane is fit through the rosette portion of the minimized aggregate so that the sum of squared distances from that plane is minimized. The distance of all nonhydrogen atoms of the M and CA groups from the plane is measured and DP is calculated using Equation (8).

$$\text{DP} = \left[\frac{\left(\sum_{i=1}^N (\Delta r_i)^2 \right)}{N} \right]^{1/2} \quad (8)$$

where Δr is the distance of an atom from the plane and N is the number of atoms in the rosette. Large values of DP correspond to rosettes that are more bowl-shaped; small values of DP correspond to rosettes that are more planar (Figure 12). The values of DP correlate with experimentally determined stabilities for $\text{hub(M)}_3 \cdot 3\text{CA} > \text{triaz(M)}_3 \cdot 3\text{CA}$ and $\text{Ad(M)}_3 \cdot 3\text{CA} > \text{flex(M)}_3 \cdot 3\text{CA}$: the larger the value of DP, the lower the stability of the aggregate.

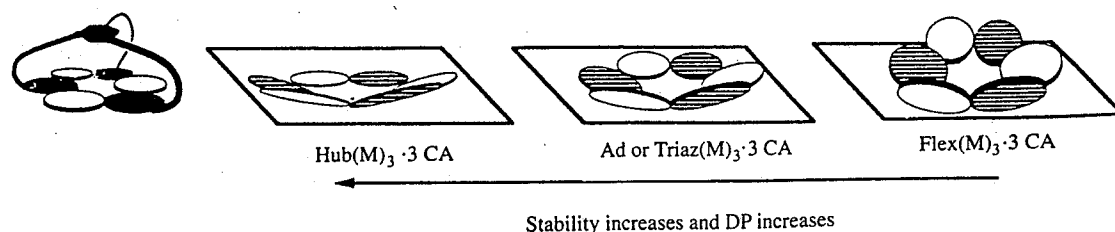


Figure 12 The stability of aggregates (determined experimentally) can be correlated to the computational parameter, DP, that describes the distortion of the heavy atoms of CA and M from a mean plane. The most stable aggregate (left) shows the most planar rosette after minimization (small DP). The least stable aggregate (right) shows the most bowled rosette after minimization (large DP). Both triaz(M)_3 and ad(M)_3 yield comparable values of DP and are of comparable stability. The bowling of the rosettes is shown crudely: for a more rigorous diagram, please see the original source (Ref. 19).

17.5.3.2 The role of solvent

Initial simulations carried out for (2) in vacuum resulted in a structure that was inconsistent with the ^1H NMR spectra: symmetry was lost due to strong interactions between the three amides of the central hub and portions of the rosette. The aggregate collapsed upon itself. Simulations done in chloroform, with one molecule of chloroform placed within the central cavity of the aggregate (between the rosette and hub portions), resulted in structures more consistent with the ^1H NMR spectrum—and more similar to the starting structure than those without solvent. For the timescale of the experiment (80 ps), no significant diffusion of molecules of chloroform away from the aggregate was observed. Of all the molecules of chloroform in the simulation, four interacted most strongly: the caged chloroform and one between each of the three spokes. The trend in value of DP for an abbreviated (and faster) minimization strategy including only these four chloroform molecules showed the same trend in stability.

17.5.4 Theory

One goal of this project has been to develop an intuitive sense for the design of aggregates and their stabilities. This strategy requires an understanding of the balance between enthalpic gains resulting from the formation of hydrogen bonds, and entropic costs from the aggregation of independent particles. Ideally we would like to be able to estimate ΔG , or a surrogate of it. To accomplish this goal, we require simple estimates of ΔH and ΔS .

17.5.4.1 The number of hydrogen bonds (HB) is proportional to the enthalpy of aggregation (ΔH)

The total enthalpy of assembly can be described as the sum of hydrogen bonds and van der Waals forces (Equation (9); no ionic or charge-charge interactions exist in these aggregates). Since recognition occurs in organic solvents, we believe that the contribution of van der Waals interactions to the stability of an aggregate is minimal—that is, organic molecules show little preference for contact with molecules of solvent or molecules of solute. If all the hydrogen bonds have equal energy, or are identical in the aggregates compared (i.e., while the hydrogen bonds of a rosette are likely to be different in strength, the contribution of an entire rosette should be constant), the total enthalpy of aggregation should be proportional to the number of hydrogen bonds (HB).

$$\Delta H = \Delta H_{\text{HB}} + \Delta H_{\text{vdw}} = \text{HB} \quad (9)$$

17.5.4.2 The number of particles is proportional to the entropy of aggregation

Equations (6) and (7) describe the rotational and translational entropies of aggregation. In both cases, the total entropy is proportional to $(N-1)$. Estimating the contribution of conformational entropy is difficult. If the molecules that are being compared have similar connectivities, then this component can be ignored. While this approximation limits the generality of any subsequent model, models that rationalize stabilities have emerged.

$$\Delta S = (N-1) \quad (10)$$

Estimating ΔG using Equations (9) and (10) yields Equations (11)–(13). This expression is of limited use because the constants c_1 and c_2 cannot be easily evaluated and may be system dependent. If we choose to evaluate these expressions as described by Equation (13), a situation suggesting a melting process is implied: this melting can be examined experimentally by titrations of solutions of aggregates with methanol.

$$\Delta G = \Delta H - T\Delta S \quad (11)$$

$$\Delta G = c_1 \text{HB} - c_2 T\Delta S \quad (12)$$

$$(c_2/c_1)T = \text{HB}/(N-1) \quad (13)$$

While evaluating the constant terms and solving Equation (12) rigorously would be preferred, $HB/(N-1)$ is qualitatively useful: it seems to correlate with stability. Values for $HB/(N-1)$ are given in Table 4 for a number of aggregates.

17.6 CRYSTALLINE SOLIDS

Our discussion of crystalline solids based on CA·M is divided into three parts. Section 17.6.1 describes our motivations for this study. Section 17.6.2 introduces our studies of crystalline materials and discusses representative crystal structures. Section 17.6.3 summarizes the conclusions we can so far draw from our efforts with this system.

17.6.1 Crystal Engineering

The phrase "crystal engineering" describes both the effort to rationalize the relationship between the structure of molecules and the structures of the crystals that form from them, and the attempt to use this information to design molecules that will pack in desired crystal structures. The strategy that we have adopted—a strategy that has been used by many others including Etter and co-workers,²⁰ Leiserowitz and co-workers,²¹ Taylor and Kennard,²² Jeffrey and Saenger,²³ Bishop and Dance,²³ Hsu and Craven,²³ and Shimizu *et al.*²³—is to use directional interactions such as hydrogen bonds to impose constraints on the packing arrangement.

Many enthalpic constraints have been identified and used successfully: repulsive van der Waals forces prevent energetically unfavorable close contacts; attractive van der Waals interactions tend to bring molecules into arrangements that minimize the free volume of the crystal; specific interactions—hydrogen bonds,²⁴ charge–charge,²⁵ dipole–induced dipole,²⁶ and charge transfer²⁷—orient molecules in specific arrangements. The magnitude of the enthalpic gain from engineering these forces into a crystalline architecture must exceed the entropic costs associated with that specific packing arrangement: vibrational motion and conformational freedom of the molecules influences the packing arrangement in unpredictable and nonintuitive ways.

Although there is some progress both experimentally and theoretically,²⁸ prediction of a crystal structure based on the structures of the component molecule(s) is impossible. In an effort to simplify the problem, there has been a substantial focus on the design and development of specific architectures based on directional interactions: tapes,²⁹ sheets,³⁰ and diamondoid³¹ structures have been investigated most thoroughly. These motifs limit the range of possible arrangements of the molecules in space and begin to reduce the dimensionality of the problem—that is, the ability to predict how two-dimensional sheets stack to form a three-dimensional crystal would represent a substantial contribution to this field.

Our work has focused on tapes comprising 1:1 cocrystals of CA and M: we have observed both linear and crinkled tapes derived from the CA·M lattice. Here we will summarize only the broad features of this work, and will emphasize information relevant to the idea that the CA·M lattice can be considered a scaffold for the design in the solid state as well as design in solution. We now believe that the problem in rationalization posed by this system, although simpler than that for an arbitrary organic molecule without constraints, is still too complex to be solved at the current state of the science in this area. The problem of polymorphism attributable (at least in part) to rotational isomers around the *N*-phenyl bond and the ethyl groups of diethylbarbituric acid is a particular problem that has proved intractable, although it may be possible to use molecules with substituents chosen to eliminate the conformational isomerism that results from these groups.

17.6.2 Motifs and Structure

Three motifs can be obtained from the cocrystallization of CA and M: rosettes and linear or crinkled tapes.^{32–5} These motifs arise from different connectivities of CA and M. The pattern of connectivity is highly dependent on the size of the groups on the periphery: peripheral crowding is an effective strategy for design in the solid state.

17.6.2.1 Linear tapes: small peripheral groups

The majority of crystalline tapes that we have obtained are linear. When the peripheral groups are small (Figure 13), linear tapes appear to be favored over crinkled tapes and rosettes, although for no

obvious reason. We have obtained tapes from two related series of molecules: the cocrystallization of 5,5-diethylbarbituric acid with any of seven *N, N'*-bis(*p*-X-phenyl)melamines (X = H, F, Cl, Br, I, Me, and CF₃) or any of four *N, N'*-bis(*m*-X-phenyl)melamines (X = F, I, Me, and CF₃).³³ Four additional complexes also form linear tapes (Figure 14).³⁴ These last four were pursued to assess opportunities for secondary interactions (R—I...NC—R), to observe what happened in the absence of peripheral groups, and to determine the propensity of imperfect molecules to form tapes.

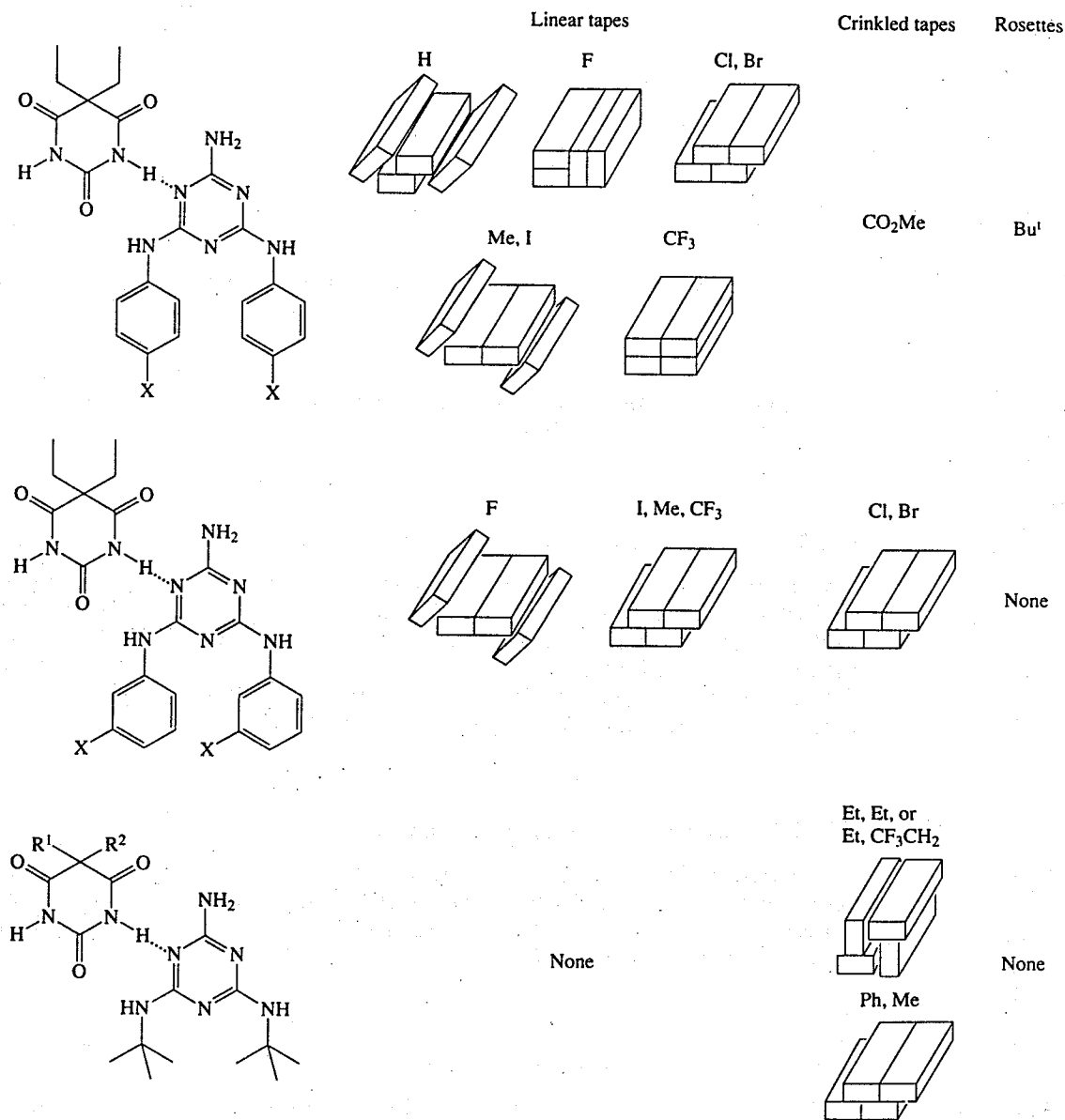


Figure 13 Linear tapes, crinkled tapes, and rosettes are classified based on the structures of the molecules comprising them. In all cases, tapes pack with their long axes (the hydrogen-bonded axis) parallel (long edge of the block). The block diagrams serve to communicate crudely the three-dimensional packing of these tapes. Similar arrangements do not imply polymorphism: the crystal structures are less similar than these diagrams imply.

With one exception, all tapes lie with their long axes parallel. The packing of linear tapes shows no simple trend with the size of the groups on the periphery. Figures 13 and 14 attempt to represent some of this diversity. Translations in all three dimensions make these structures even less similar: only one isomorphous pair exists (Br and Cl). Generalizations about the role of

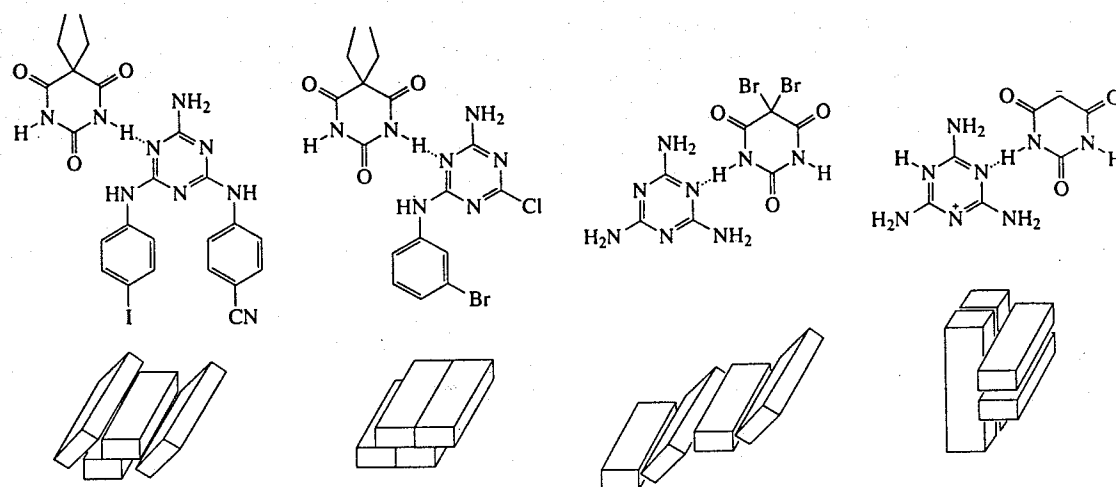


Figure 14 Linear tapes resulted from the crystallization of the molecules shown. In one instance, the tape axes did not align parallel.

peripheral groups can be made, but the complexity of these molecules and polymorphism (discussed later) complicate these issues.

17.6.2.2 Crinkled tapes: medium-sized peripheral groups

When the size of the substituents on the melamines is increased, crinkled tapes are observed: 5,5-diethylbarbituric acid and *N,N'*-bis(4-*X*-phenyl)melamines (*X* is CO₂-Me) yield crinkled tapes, while *X* < CF₃ yields linear tapes (Figure 13).³⁵ Crinkled tapes are obtained from 1:1 complexes between *N,N'*-di(*t*-butyl)melamine and 5,5-disubstituted barbituric acids (diethyl, dimethyl, diphenyl, ethyltrifluoroethyl). While the crinkling of one tape may effect the packing of its neighbor, no general trends emerge about the relative structure of these tapes.

17.6.2.3 Rosette: large peripheral groups

If the size of the peripheral group is further increased (as shown in Figure 12), the infinite crinkled tape structure is replaced by the rosette. We have been able to obtain only one crystal structure of a rosette: the 1:1 complex of *N,N'*-bis(4-*t*-butyl phenyl)melamine and 5,5-diethyl barbital. The crystal structure is shown in Figure 15.¹⁵

17.6.3 Implications for Crystal Engineering

While the synthetic accessibility to a large number of substituted melamines and barbiturates makes this system attractive, many issues suggest that CA·M is not the system of choice for these studies.

17.6.3.1 Cocrystallization is difficult

The tapes based on cyanuric acid (barbital) and melamine lattices are difficult to crystallize. Growing crystals of the quality and size suitable for single-crystal x-ray diffraction requires patience. Crystal growth is favored kinetically along the tape axis (in the direction that leads to new hydrogen-bond formation): crystals obtained are usually needles that are too thin to be used for single-crystal x-ray diffraction study.

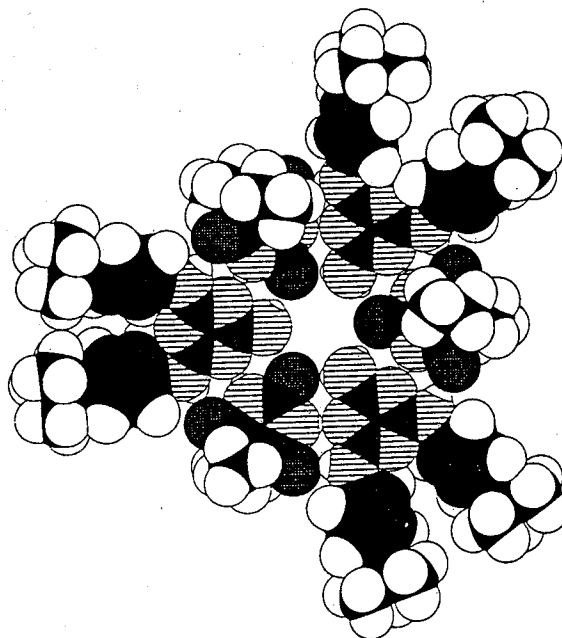


Figure 15 The crystal structure of the rosette. Carbon atoms are black. Hydrogen atoms are white. Nitrogen atoms are striped. Oxygen atoms are hatched.

17.6.3.2 Conformational complexity and polymorphism

The number of ways that molecules of CA and M can arrange their peripheral groups while maintaining the same tape motif leads to the existence of polymorphs. Orientations of the ethyl groups of diethylbarbital and free rotation along the *N*-phenyl bond is probably responsible for polymorphism in the CA·M system.

17.6.3.3 The utility of powder diffraction

One of the key concerns in efforts to develop a rational understanding of the organic solid state is the unpredictable, but substantial, occurrence of polymorphism. The crystal structure obtained in any single-crystal study could be a true minimum energy structure, or a local minimum, or a metastable phase formed kinetically under the conditions of a specific crystallization. To survey for polymorphism, we have relied on x-ray powder diffraction (XPD). XPD performed on powders of mixtures of CA and M from different solvents (such as acetone, MeCN, THF-CHCl₃, and MeOH) has led us to believe that a majority of the reported structures are minimum energy structures. Using XPD we were, however, able to determine that the tape from *N,N'*-bis(*P*-bromophenyl)melamine does crystallize in two different structures. By comparison of the XPD patterns calculated based on the single-crystal coordinates with the experimental XPD patterns from the powders obtained from different solvents suggest that one of the polymorphs is isomorphous to the X = Cl complex, the other is related to the X = Me complex.

17.7 CONCLUSIONS

CA·M is a useful platform for the construction of soluble aggregates and crystalline materials, although its use for exploring the latter is limited by the low solubility of the components, by the difficulties of cocrystallization, and by the complexities of polymorphism and structural isomerism. The greatest benefit from efforts with this system is the observation that important principles which emerge from the solid state also seem relevant to solution-based design. The most important of these is the value of steric effects (peripheral crowding) in excluding structures: if one wishes a particular structure not to form, it may be possible to exclude it by arranging substituents in a way that make it sterically unfavorable. This strong conceptual complementarity is a strong motivation to us, and others,³⁶ for pursuing this system.

Exploration of the CA-M system provides trials of techniques of characterization useful for the study of noncovalent systems. While these techniques are not new to the community of organic chemists, their application to this class of compounds has suggested both their strengths and weaknesses. GPC, VPO, and ESI-MS will undoubtedly prove useful to others in the community. Additional techniques are being surveyed: analysis of limited regions of the ^1H NMR spectra is proving to be both useful and general.

The most significant contribution of this work to date is the generation of a data set: we have constructed more than 20 different aggregates based on the rosette. With this data set we can begin exploring the use of computation and theory for more efficient design. The use of computation to rationalize stabilities and to aid in design remains in its early stages, although the surrogate for stability, DP, appears to be general to many of these aggregates based on monorosettes. This set of data sharpens intuition about the balance between enthalpy and entropy in these systems. A useful result is rule-of-thumb: increased stability correlates with higher values of $\text{HB}/(N-1)$.

ACKNOWLEDGMENTS

This work was supported by the NSF grant CHE-91-2233 1. EES gratefully acknowledges Eli Lilly for a predoctoral fellowship (1995). Much of the work reported on aggregates in solution was carried out by Drs. Christopher Seto, John Mathias, and Dana Gordon. Dr. Donovan Chin performed the computational work. Mathai Mammen contributed to the section on theory. Dr. Mohammed I. M. Wazeer assisted with NMR analysis of isomerism. Work in the solid state was done by Drs. Jonathon Zerkowski and John MacDonald.

17.8 REFERENCES

1. M. Mrksich and P. B. Dervan, *J. Am. Chem. Soc.*, 1995, 117, 3325.
2. S. L. Schreiber, *Science*, 1991, 251, 283.
3. D. H. Williams, M. S. Searle, J. P. Mackay, U. Gerhard, and R. A. Maplestone, *Proc. Natl. Acad. Sci. USA*, 1993, 90, 1172.
4. C. J. Pedersen, *Angew. Chem., Int. Ed. Engl.*, 1988, 27, 1021 and references cited therein.
5. D. J. Cram, *Angew. Chem., Int. Ed. Engl.*, 1988, 27, 1009.
6. J. M. Lehn, *Angew. Chem., Int. Ed. Engl.*, 1988, 27, 89.
7. References for these ion receptors are identified by the investigator as denoted in the Figure. (Ionomycin) B. K. Toepfritz, A. I. Cohen, P. T. Funke, W. L. Parker, and J. Z. Gougoutas, *J. Am. Chem. Soc.*, 1979, 101, 3344; (Lehn) B. Dietrich, M. W. Hosseini, J. M. Lehn, and R. B. Sessions, *J. Am. Chem. Soc.*, 1981, 103, 1282; (Pederson) See Ref. 4; (Raymond) T. D. Y. Chung and K. N. Raymond, *J. Am. Chem. Soc.*, 1993, 115, 6765; (Reinhoudt) D. M. Rudkevich, W. Verboom, Z. Brzozka, M. C. Palys, W. P. R. V. Staathamer, G. J. van Hummel, S. M. Franken, S. Harkema, J. F. J. Engbersen, and D. N. Reinhoudt, *J. Am. Chem. Soc.*, 1994, 116, 4341; (Schmidtchen) F. P. Schmidtchen, *J. Am. Chem. Soc.*, 1986, 108, 8249 and references therein; (Shinkai) H. Yamamoto and S. Shinkai, *Chem. Lett.*, 1994, 1115; (Vogtle) J. Gross, G. Harder, F. Vogtle, H. Stephan, and K. Gloe, *Angew. Chem., Int. Ed. Engl.*, 1995, 34, 481.
8. References for these small molecule receptors are identified by the investigator as denoted in the Figure. (Bell) T. W. Bell and J. Liu, *J. Am. Chem. Soc.*, 1988, 110, 3673; (Breslow) J. M. Desper and R. Breslow, *J. Am. Chem. Soc.*, 1994, 116, 12081; (Cram) C. N. Eid, Jr., C. B. Knobler, D. A. Gronbeck, and D. J. Cram, *J. Am. Chem. Soc.*, 1994, 116, 8506; (Diederich) B. R. Peterson, T. Morasini-Denti, and F. Diederich, *Chem. Biol.*, 1995, 2, 139; (Hamilton) S.-K. Chang, D. Van Engen, E. Fan, and A. D. Hamilton, *J. Am. Chem. Soc.*, 1991, 113, 7640; (Hunter) C. A. Hunter, *J. Chem. Soc., Chem. Commun.* 1991, 749; (Kelly) T. R. Kelly and M. P. Maguire, *J. Am. Chem. Soc.*, 1987, 109, 6549; (Koga) K. Odashima, A. Itai, Y. Iitaka, and K. Koga, *J. Am. Chem. Soc.*, 1980, 102, 2504; (de Mendoza and Rebek) R. Wyler, J. de Mendoza, and J. Rebek, *Angew. Chem., Int. Ed. Engl.*, 1993, 32, 1699; (Rebek) J. Rebek, K. Williams, K. Parris, P. Ballester, and K. S. Jeong, *Angew. Chem., Int. Ed. Engl.*, 1987, 26, 1244; (Still) K. T. Chapman and W. C. Still, *J. Am. Chem. Soc.*, 1989, 111, 3075; S.-S. Yoon and W. C. Still, *J. Am. Chem. Soc.*, 1993, 115, 823; (Reinhoudt) P. Timmerman, W. Verboom, F. C. J. M. van Veggel, W. P. van Hoorn, and D. N. Reinhoudt, *Angew. Chem. Int. Ed. Engl.*, 1994, 33, 2345; (Whitlock) J. E. Cochran, T. J. Parrott, B. J. Whitlock and H. W. Whitlock, *J. Am. Chem. Soc.*, 1992, 114, 2269; (Zimmerman) S. C. Zimmerman, C. M. Vanzyl, and G. S. Hamilton, *J. Am. Chem. Soc.*, 1989, 111, 1373.
9. References for these molecular machines are identified by Equations. (a) Equation (1) R. A. Bissell, E. Cordova, A. E. Kaifer, and J. F. Stoddart, *Nature*, 1994, 369, 133; (b) Equation (2) L. Zelikovich, J. Libman, and A. Shanzer, *Nature* 1995, 374, 790.
10. References for these scaffolds are identified by the investigator as denoted in the Figure. (Ghadiri) M. R. Ghadiri, K. Kobayashi, J. R. Granja, R. K. Chadha, and D. E. McRee, *Angew. Chem., Int. Ed. Engl.*, 1995, 34, 93 and references therein; (Lehn) P. N. W. Baxter, J. M. Lehn, J. Fischer, and M. T. Youinou, *Angew. Chem., Int. Ed. Engl.*, 1994, 33, 2284; (Sauvage) C. O. Dietrich-Buchecker and J. P. Sauvage, *Chem. Rev.*, 1987, 87, 798; (Stoddart) D. B. Amabilino, P. R. Ashton, A. S. Reder, N. Spencer, and J. F. Stoddart, *Angew. Chem., Int. Ed. Engl.*, 1994, 33, 1286; (Seeman) J. Chen and N. C. Seeman, *Nature*, 1991, 350, 631; (Whitesides) G. M. Whitesides, E. E. Simanek, J. P. Mathias, C. T. Seto, D. Chin, M. Mammen, and D. M. Gordon, *Acc. Chem. Res.*, 1995, 28, 37.
11. R. Taylor and O. Kennard, *Acc. Chem. Res.*, 1984, 17, 320 and references therein.

12. Aggregate (1): J. P. Mathias, E. E. Simanek, J. A. Zerkowski, C. T. Seto, and G. M. Whitesides, *J. Am. Chem. Soc.*, 1994, 116, 4316; Aggregate (2): C. T. Seto and G. M. Whitesides, *J. Am. Chem. Soc.*, 1993, 115, 905; Aggregate (3) C. T. Seto and G. M. Whitesides, *J. Am. Chem. Soc.*, 1993, 115, 1330; Aggregate (4): J. P. Mathias, E. E. Simanek, and G. M. Whitesides, *J. Am. Chem. Soc.*, 1994, 116, 4326; Aggregates (5) and (6): J. P. Mathias, C. T. Seto, E. E. Simanek, and G. M. Whitesides, *J. Am. Chem. Soc.*, 1994, 116, 1725; Aggregate (7): C. T. Seto and G. M. Whitesides, *J. Am. Chem. Soc.*, 1991, 113, 712; C. T. Seto, J. P. Mathias, and G. M. Whitesides, *J. Am. Chem. Soc.*, 1993, 115, 1321; Aggregate (8): reported with (5) and (6); Aggregate (9): J. P. Mathias, E. E. Simanek, C. T. Seto and G. M. Whitesides, *Angew. Chem., Int. Ed. Engl.*, 1993, 32, 1766.
13. R. C. Helgeson, B. J. Selle, I. Goldberg, C. B. Knobler and D. J. Cram, *J. Am. Chem. Soc.*, 1993, 115, 11 506.
14. D. A. McQuarrie, "Statistical Thermodynamics," Harper & Row, New York, 1973, chaps. 5 and 6.
15. J. A. Zerkowski, C. T. Seto, and G. M. Whitesides, *J. Am. Chem. Soc.*, 1992, 114, 5473.
16. X. Cheng, Q. Gao, R. D. Smith, E. E. Simanek, M. Mammen and G. M. Whitesides, *Rapid Commun. Mass Spectrom.*, 1995, 9, 312; For an alternative strategy see: K. C. Russell, E. Leize, A. V. Dorsselaer, and J. M. Lehn, *Angew. Chem., Int. Ed. Engl.*, 1995, 34, 209.
17. Determining stability by doing titrations with methanol focuses on the kinetic stability of these aggregates. We have not thoroughly examined all the aggregates to determine whether this trend in stability is identical to the desired trend in thermodynamic stability. We are currently pursuing these studies.
18. E. E. Simanek, M. I. M. Wazeer, J. P. Mathias, and G. M. Whitesides, *J. Org. Chem.*, 1994, 59, 4904.
19. Full details of our efforts in applying computation to these systems can be found in: D. N. Chin, D. M. Gordon, and G. M. Whitesides, *J. Am. Chem. Soc.*, 1994, 116, 12 033; X. Li, D. N. Chin, and G. M. Whitesides, *J. Org. Chem.*, 1996, 61, 1779.
20. M. C. Etter, K. S. Hung, G. M. Frankenbach, and D. A. Adsmond, in "Materials for Nonlinear Optics: Chemical Perspectives," eds. S. R. Marder, J. E. Sohn, and G. D. Stucky, American Chemical Society, Washington, DC, 1991, vol. 455, p. 446; M. C. Etter, G. M. Frankenbach, and D. A. Adsmond, *Mol. Cryst. Liq. Cryst.*, 1990, 187, 25; M. C. Etter, *Acc. Chem. Res.*, 1990, 23, 120.
21. L. Leiserowitz and G. M. J. Schmidt, *J. Chem. Soc. (A)*, 1969, 2372; L. Leiserowitz and F. Nader, *Acta Crystallogr., Sect. B*, 1977, 33, 2719; L. Leiserowitz and M. Tuval, *Acta Crystallogr., Sect. B*, 1978, 34, 1230; S. Weinstein, L. Leiserowitz, and E. Gil-Av, *J. Am. Chem. Soc.*, 1980, 102, 2768.
22. R. Taylor and O. Kennard, *J. Am. Chem. Soc.*, 1982, 104, 5063.
23. G. A. Jeffrey and W. Saenger, "Hydrogen Bonding in Biological Structures," Springer, Berlin, 1991; R. Bishop and I. G. Dance, in "Inclusion Compounds," eds. J. L. Atwood, D. D. MacNicol and J. E. D. Davies, Academic Press, London, 1991, vol. IV; I. Hsu and B. M. Craven, *Acta Crystallogr., Sect. B*, 1974, 30, 974; N. Shimizu, S. Nishigaki, Y. Nakai, and K. Osaki, *Acta Crystallogr., Sect. B*, 1982, 38, 2309.
24. C. B. Aakeroy and K. R. Seddon, *Chem. Soc. Rev.*, 1993, 397; M. C. Etter, *J. Phys. Chem.*, 1991, 95, 4601; G. R. Desiraju, "Crystal Engineering: The Design of Organic Solids," Elsevier, New York, 1989; M. C. Etter, *J. Phys. Chem.*, 1991, 95, 4601.
25. U. Zimmerman, G. Schnitzler, N. Karl, E. Umbach, and R. Dudde, *Thin Solid Films*, 1989, 175, 85; E. A. Sudbeck and M. C. Etter, *Chem. Mater.*, 1994, 6, 1192; M. C. Grossel, P. B. Hitchcock, K. R. Seddon, T. Welton, and S. C. Weston, *Chem. Mater.*, 1994, 6, 1106.
26. D. S. Reddy, K. Panneerselvam, T. Pilati, and G. R. Desiraju, *J. Chem. Soc., Chem. Commun.*, 1993, 661.
27. P. J. Fagan, M. D. Ward, and J. C. Calabrese, *J. Am. Chem. Soc.*, 1989, 111, 1698; M. D. Ward, P. J. Fagan, J. C. Calabrese, and D. C. Johnson, *J. Am. Chem. Soc.*, 1989, 111, 1719.
28. J. Perlstein, *J. Am. Chem. Soc.*, 1994, 116, 455; J. Perlstein, *Chem. Mater.*, 1994, 6, 319; A. Gavezzotti, *J. Am. Chem. Soc.*, 1991, 113, 4622.
29. J. C. MacDonald and G. M. Whitesides, *Chem. Rev.*, 1994, 94, 2383; M. W. Hosseini, T. Ruppert, P. Shaeffer, A. Decian, N. Kyritsakas, and J. Fischer, *J. Chem. Soc. Chem. Commun.*, 1994, 2135; E. Fan, J. Yang, S. B. Geib, T. C. Stoner, M. D. Hopkins, and A. D. Hamilton, *J. Chem. Soc. Chem. Commun.*, 1994, 1251.
30. D. S. Reddy, B. S. Goud, K. Panneerselvam, and G. R. Desiraju, *J. Chem. Soc., Chem. Commun.*, 1993, 663. Y.-L. Chang, M.-A. West, F. W. Fowler, and J. W. Lauher, *J. Am. Chem. Soc.*, 1993, 115, 5991; M. D. Hollingsworth, M. E. Brown, B. D. Santarsiero, J. C. Huffman, and C. R. Goss, *Chem. Mater.*, 1994, 6, 1227. V. A. Russel, M. C. Etter, and M. D. Ward, *J. Am. Chem. Soc.*, 1994, 116, 1941; K. D. M. Harris and M. D. Hollingsworth, *Nature*, 1989, 341, 19.
31. M. Simard, D. Su, and J. D. Wuest, *J. Am. Chem. Soc.*, 1991, 113, 4696; X. Wang, M. Simard, and J. D. Wuest, *J. Am. Chem. Soc.*, 1990, 116, 12119; O. Ermer, *J. Am. Chem. Soc.*, 1988, 110, 3747; O. Ermer and A. Eling, *J. Chem. Soc. Perkin Trans. 2*, 1994, 925; D. S. Reddy, D. C. Craig, A. D. Rae, and G. R. Desiraju, *J. Chem. Soc., Chem. Commun.*, 1993, 1737; M. J. Zaworotko, *Chem. Soc. Rev.*, 1994, 23, 283.
32. J.-M. Lehn, M. Mascal, A. DeCian, and J. Fischer, *J. Chem. Soc., Chem. Commun.*, 1990, 479.
33. (Linear) J. A. Zerkowski, J. C. MacDonald, C. T. Seto, D. A. Wierda, and G. M. Whitesides, *J. Am. Chem. Soc.*, 1994, 116, 2382; J. A. Zerkowski and G. M. Whitesides, *J. Am. Chem. Soc.*, 1994, 116, 4298; (Linear and crinkled) J. A. Zerkowski, J. P. Mathias, and G. M. Whitesides, *J. Am. Chem. Soc.*, 1994, 116, 4305.
34. J. A. Zerkowski, J. C. MacDonald, and G. M. Whitesides, *Chem. Mater.*, 1994, 6, 1250.
35. J. A. Zerkowski, C. T. Seto, and G. M. Whitesides, *J. Am. Chem. Soc.*, 1990, 112, 9025. See also Refs. 16 and 34.
36. See for example: K. Matsharei and D. C. Myles, *J. Am. Chem. Soc.*, 1994, 116, 7413, N. Kimizuka, T. Kawasaki, K. Hirata, and T. Kunitake, *J. Am. Chem. Soc.*, 1995, 117, 6360.

ful for the
of organic
ngths and
mmunity.
spectra is

we have
can begin
utation to
rogate for
This set of
. A useful

nowledges
n solution
van Chin
on theory.
solid state

S.A., 1993, 90,

nycin) B. K.
44; (Lehn) B.
a) See Ref. 4;
. Rudkevich,
arkema, J. F.
chen, *J. Am.*
., 1994, 1115;
44, 481.
(Bell) T. W.
n. *Soc.*, 1994,
c., 1994, 116,
milton) S.-K.
A. Hunter, *J.*
37, 109, 6549;
a and Rebek)
K. Williams,
an and W. C.
(Reinhoudt)
Chem. Int. Ed.
i. *Chem. Soc.*,
c., 1989, 111,

ordova, A. E.
anzer, *Nature*

. Ghadiri, K.
and references
ngl., 1994, 33,
B. Amabilino,
5; (Seeman) J.
Mathias, C. T.

